Early Actinide Alkoxide Chemistry. Synthesis, Characterization, and Molecular Structures of Th(IV) and U(IV) Aryloxide Complexes

John M. Berg,[1a] David L. Clark,*[,1b] John C. Huffman,[1c] David E. Morris,[1a] Alfred P. Sattelberger,*[,1d] William E. Streib,[1c] William G. Van Der Sluys,[1a,e] and John G. Watkin[1a]

Contribution from the Isotope and Nuclear Chemistry Division, Los Alamos National Laboratory, Los Alamos, New Mexico 87545, and Molecular Structure Center, Department of Chemistry, Indiana University, Bloomington, Indiana 47401. *Received May 22, 1992*

Abstract: Several synthetic procedures have been developed for the preparation of early actinide aryloxide complexes. Simple alcoholysis of the actinide metallacycle $\{[(Me_3Si)_2N]_2An(CH_2SiMe_2NSiMe_3)\}$ [An = Th (**1**), U (**2**)] using 1 equiv of 2,6-disubstituted phenol results in the protonation of the An–C bond to form mono(aryloxide) complexes $An(O\text{-}2,6\text{-}R_2C_6H_3)[N(SiMe_3)_2]_3$ [An = U; R = *t*-Bu (**3**), *i*-Pr (**4**). An = Th; R = *t*-Bu (**5**), Me (**6**)] in essentially quantitative yield. For An = Th, further stepwise substitution products, the bis(aryloxide) or tris(aryloxide) complexes $Th(O\text{-}2,6\text{-}t\text{-}Bu_2C_6H_3)_2[N(SiMe_3)_2]_2$ (**7**) and $Th(O\text{-}2,6\text{-}t\text{-}Bu_2C_6H_3)_3[N(SiMe_3)_2]$ (**8**), are readily isolated depending on the stoichiometry of added phenol. Prolonged (36 h) reflux with excess 2,6-di-*tert*-butylphenol fails to provide the homoleptic $Th(O\text{-}2,6\text{-}t\text{-}Bu_2C_6H_3)_4$ via this simple protonolysis reaction. Thorium metallacycle **1** reacts with 4 equiv of HO-4-*t*-BuC_6H_4 to produce polymeric $[Th(O\text{-}4\text{-}t\text{-}BuC_6H_4)_4]_x$, addition of pyridine to which yields the monomeric adduct $Th(O\text{-}4\text{-}t\text{-}BuC_6H_4)_4(py)_3$ (**10**). For alcoholysis reactions employing the uranium metallacycle (**2**), addition of slightly greater than 4 equiv of HO-2,6-*t*-$Bu_2C_6H_3$ in refluxing toluene for 6 h provides $U(O\text{-}2,6\text{-}R_2C_6H_3)_4$ [R = *t*-Bu (**11**), *i*-Pr (**12**)]. While alcoholysis fails to provide the homoleptic $Th(O\text{-}2,6\text{-}t\text{-}Bu_2C_6H_3)_4$ (**9**), we can prepare this complex via a metathetical procedure. Reaction of $ThI_4(THF)_4$ with 4 equiv of KO-2,6-*t*-$Bu_2C_6H_3$ in THF provides **9** in high yield. For less sterically-demanding aryloxide ligands, metathesis of $ThI_4(THF)_4$ with 4 equiv of KO-2,6-$R_2C_6H_3$ in THF results in formation of bis(THF) adducts $Th(O\text{-}2,6\text{-}R_2C_6H_3)_4(THF)_2$ [R = Me (**13**), *i*-Pr (**14**)]. The THF adducts readily exchange with pyridine to give $Th(O\text{-}2,6\text{-}Me_2C_6H_3)_4(py)_2$ (**15**). These new aryloxide compounds have been characterized by elemental analysis, ^1H NMR, infrared spectroscopy, and, for $U(O\text{-}2,6\text{-}t\text{-}Bu_2C_6H_3)[N(SiMe_3)_2]_3$ (**5**), $An(O\text{-}2,6\text{-}t\text{-}Bu_2C_6H_3)_4$, [An = Th (**9**), U (**11**)], and $Th(O\text{-}2,6\text{-}Me_2C_6H_3)_4(py)_2$ (**15**), single-crystal X-ray diffraction. In **5**, the U metal center is coordinated to the O atom of the aryloxide ligand and the N atoms of the three silylamide ligands, in a pseudotetrahedral fashion with U–O and U–N distances of 2.145 (8) and 2.285 (11) Å, respectively. $An(O\text{-}2,6\text{-}t\text{-}Bu_2C_6H_3)_4$ complexes (An = Th, U) are isostructural and possess crystallographic S_4 symmetry. Each set of four An–O bond lengths is identical [2.189 (6) Å, Th; and 2.135 (4) Å, U], and the O–An–O angles are of two types, four of 110.46 (15)° for An = Th [110.2 (1)°, An = U] and two of 107.5 (3)° for An = Th [108.0 (2), An = U], and correspond to a slight flattening of the central AnO_4 core. **15** has a pseudo-octahedral geometry about the central Th atom with the two pyridine ligands occupying cis positions. The average Th–N and Th–O distances are respectively 2.679 and 2.198 Å. Crystal data for **5** (−155 °C): orthorhombic space group $P2_12_12_1$; a = 11.257 (3), b = 19.761 (6), c = 19.589 (7) Å; V = 4357.46 Å^3; d_{calc} = 1.409 g cm^{-3}; Z = 4. **9** (−171 °C): tetragonal space group $I\bar{4}$; $a = b$ = 14.082 (5), c = 13.468 (5) Å; V = 2670.75 Å^3; d_{calc} = 1.317 g cm^{-3}; Z = 2. **11** (−145 °C): tetragonal space group $I\bar{4}$; $a = b$ = 14.066 (2), c = 13.404 (2) Å; V = 2652.10 Å^3; d_{calc} = 1.327 g cm^{-3}; Z = 2. **15** (−171 °C): monoclinic space group $P2_1/n$; a = 14.724 (3), b = 19.724 (3), c = 15.456 (2) Å; β = 100.95 (1)°; V = 4407.01 Å^3; d_{calc} = 1.458 g cm^{-3}; Z = 4.

Introduction

Alkoxide complexes of the actinide elements were first reported in the mid 1950's, during the search for volatile complexes for uranium isotope separation.[2-4] It is ironic that, after some 40 years of investigation, we are only now beginning to understand the rich solution, structural, and reaction chemistry of this fascinating class of actinide compounds. Much of the early work in the field of actinide alkoxide complexes was due to the pioneering efforts of Bradley and Gilman, whose groups prepared an extensive series of tetravalent actinide alkoxides of empirical formula $An(OR)_4$ (An = Th, U).[5-13] Over the last decade, however, a considerable amount of new information concerning these compounds has emerged. These recent results have helped to clear up some earlier misinterpretations of the exact nature of actinide alkoxide complexes both in solution and in the solid state.[4]

Monomeric uranium(IV) and thorium(IV) aryloxide complexes, $An(OAr)_4$, have been a synthetic goal for some time. The first well-characterized members of this class were reported by Lappert and co-workers in 1983.[14,15] Metathesis reactions of thorium or uranium tetrachloride with lithium aryloxides gave "double alkoxide" salts, $[Li(THF)_4][An(O\text{-}2,6\text{-}i\text{-}Pr_2C_6H_3)_5]$, or incomplete metathesis products such as $AnCl(O\text{-}2,4,6\text{-}t\text{-}Bu_3C_6H_2)_3$ (An = Th, U) in good yields. In the latter case, an excess of lithium aryloxide failed to provide the homoleptic early actinide complex

(1) (a) Mail Stop C346, Los Alamos. (b) Mail Stop G739, Los Alamos. (c) Indiana University. (d) Mail Stop J519, Los Alamos. (e) Present address: Department of Chemistry, The University of Montana, Missoula, MT 59812.

(2) Bradley, D. C. *Adv. Inorg. Chem. Radiochem.* **1972**, *15*, 259.

(3) Bacher, W.; Jacob, E. In *Handbook on the Physics and Chemistry of the Actinides*; Freeman, A., Keller, C., Eds.; Elsevier: Amsterdam, The Netherlands, 1985; Vol. 3, Chapter 7.

(4) (a) Sattelberger, A. P.; Van Der Sluys, W. G. *Chem. Rev.* **1990**, *90*, 1027. (b) Clark, D. L.; Sattelberger, A. P.; Van Der Sluys, W. G.; Watkin, J. G. *J. Alloys and Comp.* **1992**, *180*, 303.

(5) Bradley, D. C.; Saad, M. A.; Wardlaw, M. *J. Chem. Soc.* **1954**, 1091.

(6) Bradley, D. C.; Saad, M. A.; Wardlaw, W. *J. Chem. Soc.* **1954**, 3488.

(7) Bradley, D. C.; Chatterjee, A. K.; Wardlaw, W. *J. Chem. Soc.* **1956**, 2260.

(8) Bradley, D. C.; Chatterjee, A. K.; Wardlaw, W. *J. Chem. Soc.* **1956**, 3469.

(9) Bradley, D. C.; Sinha, R. N. P.; Wardlaw, W. *J. Chem. Soc.* **1958**, 4651.

(10) Bradley, D. C.; Kapoor, R. N.; Smith, B. C. *J. Inorg. Nucl. Chem.* **1962**, *24*, 863.

(11) Bradley, D. C.; Kapoor, R. N.; Smith, B. C. *J. Chem. Soc.* **1963**, 1022.

(12) Bradley, D. C.; Kapoor, R. N.; Smith, B. C. *J. Chem. Soc.* **1963**, 204.

(13) Jones, R. G.; Martin, G. A.; Gilman, H. *J. Am. Chem. Soc.* **1956**, *78*, 4285.

(14) Blake, P. C.; Lappert, M. F.; Taylor, R. G.; Atwood, J. L.; Zhang, H. *Inorg. Chim. Acta* **1987**, *139*, 13.

(15) Hitchcock, P. B.; Lappert, M. F.; Singh, A.; Taylor, R. G.; Brown, D. *J. Chem. Soc., Chem. Commun.* **1983**, 561.

0002-7863/92/1514-10811$03.00/0

of general formula $An(OAr)_4$. The homoleptic aryloxide complexes $Th(O\text{-}2,6\text{-}Ph_2C_6H_3)_4$ and $U(O\text{-}2,6\text{-}i\text{-}Pr_2C_6H_3)_4$, obtained from the reaction of thorium or uranium tetrachloride with 4 equiv of $LiO\text{-}2,6\text{-}Ph_2C_6H_3$ or $LiO\text{-}2,6\text{-}i\text{-}Pr_2C_6H_3$, respectively, in THF, have also been described but no structural data presented.[14,15]

Lappert and co-workers have also examined the alcoholysis reaction of the uranium amide $[U(NEt_2)_4]_2$ with excess 2,6-di-*tert*-butylphenol at room temperature.[15] This reaction was unsuccessful vis-à-vis the preparation of $U(O\text{-}2,6\text{-}t\text{-}Bu_2C_6H_3)_4$; only $U(O\text{-}2,6\text{-}t\text{-}Bu_2C_6H_3)_3(NEt_2)$ could be isolated. We have repeated this reaction in our laboratory and find that, even in refluxing toluene, the fourth diethylamide ligand is not susceptible to alcoholysis.[16] Several years ago, Dormond et al.[17] described the reactions of the uranium(IV) metallacycle[18] $\{[(Me_3Si)_2N]_2U(CH_2SiMe_2NSiMe_3)\}$ (**1**) with both HO-*t*-Bu and HO-2,6-$Me_2C_6H_3$. They observed rapid protonation of the uranium–carbon bond and isolated two complexes of general formula $U(OR)[N(SiMe_3)_2]_3$. Cleavage of uranium–nitrogen bonds was also found to occur but was not competitive with attack on the metal–carbon bond. The addition of >1 equiv of alcohol led to the formation of other uncharacterized products. This observation prompted us to reinvestigate these reactions, and we report herein a detailed description of our findings concerning the alcoholysis of $\{[(Me_3Si)_2N]_2An(CH_2SiMe_2NSiMe_3)\}$ (An = Th, U) using a range of substituted phenols. We have also discovered alternate metathetical reactions that lead to $An(OAr)_4$ complexes using potassium aryloxides. Perhaps most significantly, we present the systematic physical characterization of a series of rare four-coordinate early actinide complexes, including the structural characterization of $U(O\text{-}2,6\text{-}t\text{-}Bu_2C_6H_3)[N(SiMe_3)_2]_3$ (**3**), $An(O\text{-}2,6\text{-}t\text{-}Bu_2C_6H_3)_4$ [An = Th (**9**), U (**11**)], and the Lewis base stabilized monomer, $Th(O\text{-}2,6\text{-}Me_2C_6H_3)_4(py)_2$ (**15**) (py = NC_5H_5). A preliminary account of this work has been presented.[16]

Results and Discussion

Synthesis and Reactivity. A. Preparation of Aryloxides via Protonation of An–C or An–N Bonds. In agreement with Dormond et al.,[17] we find that the reaction of 1 equiv of 2,6-disubstituted phenols ($HO\text{-}2,6\text{-}R_2C_6H_3$) with the thorium or uranium metallacycle $\{[(Me_3Si)_2N]_2An(CH_2SiMe_2NSiMe_3)\}$ [An = Th (**1**), U (**2**)] in hexane or toluene at room temperature for 1–12 h provides orange [An = U; R = *t*-Bu (**3**), *i*-Pr (**4**)] or colorless [An = Th; R = *t*-Bu (**5**), Me (**6**)] mono(aryloxide) complexes of formula $An(O\text{-}2,6\text{-}R_2C_6H_3)[N(SiMe_3)_2]_3$ in essentially quantitative yield, according to eq 1.

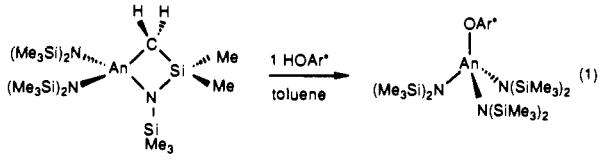

(1)

An = U, Ar* = 2,6-t-Bu2C6H3 (3), 2,6-i-Pr2C6H3 (4);

An = Th, Ar* = 2,6-t-Bu2C6H3 (5), 2,6-Me2C6H3 (6)

In reactions employing the thorium metallacycle (**1**), we have been able to isolate and characterize further stepwise substitution products in which one or two of the remaining silylamide ligands in $Th(O\text{-}2,6\text{-}t\text{-}Bu_2C_6H_3)[N(SiMe_3)_2]_3$ (**5**) have been substituted by aryloxides. Thus the reaction of the thorium metallacycle (**1**) with 2 or 3 equiv of 2,6-di-*tert*-butylphenol in refluxing toluene provides the bis(aryloxide) or tris(aryloxide) complexes $Th(O\text{-}2,6\text{-}t\text{-}Bu_2C_6H_3)_2[N(SiMe_3)_2]_2$ (**7**) or $Th(O\text{-}2,6\text{-}t\text{-}Bu_2C_6H_3)_3[N(SiMe_3)_2]$ (**8**), as outlined in eqs 2 and 3, respectively. It is

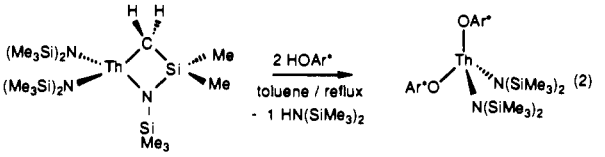

(2)

Ar* = 2,6-t-Bu2C6H3 (7)

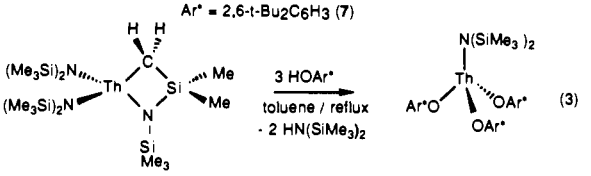

(3)

Ar* = 2,6-t-Bu2C6H3 (8)

noteworthy that, even in the presence of ≥4 equiv of HO-2,6-*t*-$Bu_2C_6H_3$, only the thorium tris(aryloxide) complex **8** can be prepared and this is readily isolated in ca. 65% crystallized yield (eq 3). Prolonged (36 h) reflux with excess 2,6-di-*tert*-butylphenol failed to yield the homoleptic thorium aryloxide of formula $Th(O\text{-}2,6\text{-}t\text{-}Bu_2C_6H_3)_4$ via this simple protonolysis reaction. We note the similarity of this result to that found by Lappert et al. for the alcoholysis reaction of $[U(NEt_2)_4]_2$ with $HO\text{-}2,6\text{-}t\text{-}Bu_2C_6H_3$ (vide supra).[15]

For alcoholysis reactions employing the uranium metallacycle **2**, addition of slightly greater than 4 equiv of $HO\text{-}2,6\text{-}R_2C_6H_3$ (R = *t*-Bu, *i*-Pr) in refluxing toluene for 6 h provides, after solvent removal and recrystallization from hexane, orange, moderately air-sensitive, crystalline $U(O\text{-}2,6\text{-}R_2C_6H_3)_4$ [R = *t*-Bu (**11**), *i*-Pr (**12**)] in 80% crystallized yield as outlined in eq 4.

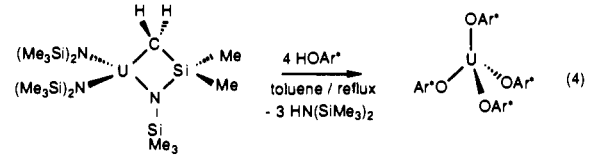

(4)

Ar* = 2,6-t-Bu2C6H3 (11), 2,6-i-Pr2C6H3 (12)

Upon decreasing the steric bulk of the substituted phenol, the reaction of the thorium metallacycle $\{[(Me_3Si)_2N]_2Th(CH_2SiMe_2NSiMe_3)\}$ (**1**) with 4 equiv of $HO\text{-}2,6\text{-}R_2C_6H_3$ (R = Me, *i*-Pr) in refluxing toluene results in *complete* protonolysis of the silylamide ligands and formation of the homoleptic aryloxide species $Th(O\text{-}2,6\text{-}R_2C_6H_3)_4$ (R = Me, *i*-Pr). Characterization of these complexes has been hampered by the insolubility of $Th(O\text{-}2,6\text{-}Me_2C_6H_3)_4$ in nondonor solvents and the great propensity of these coordinatively unsaturated complexes to pick up any trace of Lewis base (THF, pyridine, etc.) in the drybox atmosphere. Addition of 2 equiv of THF to these homoleptic aryloxide complexes results in the formation of bis(THF) adducts $Th(O\text{-}2,6\text{-}R_2C_6H_3)_4(THF)_2$ (R = Me (**13**), *i*-Pr (**14**); vide infra).

If we employ a phenol bearing no substituents in the 2,6-positions, we observe complete protonolysis of the silylamide ligands of **1** at room temperature. Thus we find that the addition of 4 equiv of 4-*tert*-butylphenol to a toluene solution of **1** at room temperature produces a white solid, insoluble in non-donor hydrocarbon solvents, which we presume to be polymeric $[Th(O\text{-}4\text{-}t\text{-}BuC_6H_4)_4]_x$. Addition of an excess of pyridine to a suspension of the solid in toluene results in complete dissolution, and upon workup from toluene the tris(pyridine) adduct $Th(O\text{-}4\text{-}t\text{-}BuC_6H_4)_4(py)_3$ (**10**) may be isolated as a white microcrystalline solid.

B. Preparation of Thorium Aryloxides via Metathetical Procedures. One of the most general synthetic routes to metal alkoxide complexes is the simple metathesis reaction of a metal halide and an alkali metal alkoxide. While this strategy has great utility in transition metal chemistry, retention of the alkali metal and formation of "ate" or "double alkoxide" complexes is a pervasive problem in actinide and lanthanide chemistry.[20] For example,

(16) Van Der Sluys, W. G.; Sattelberger, A. P.; Streib, W. E.; Huffman, J. C. *Polyhedron* **1989**, *8*, 1247.

(17) Dormond, A.; El Bouadili, A. A.; Moïse, C. J. *J. Chem. Soc., Chem. Commun.* **1985**, 914.

(18) Simpson, S. J.; Turner, H. W.; Andersen, R. A. *J. Chem. Soc.* **1979**, *101*, 7728; *Inorg. Chem.* **1981**, *20*, 2991.

(19) Turner, H. W.; Simpson, S. J.; Andersen, R. A. *J. Am. Chem. Soc.* **1979**, *101*, 2782.

Lappert and co-workers have reported metathesis reactions of thorium tetrachloride with lithium aryloxide salts which produce homoleptic aryloxide species $Th(O\text{-}2,6\text{-}Ph_2C_6H_3)_4$ and $U(O\text{-}2,6\text{-}i\text{-}Pr_2C_6H_3)_4$,[14] the "double alkoxide" complexes $[Li(THF)_4][An(O\text{-}2,6\text{-}i\text{-}Pr_2C_6H_3)_5]$ (An = Th, U),[14] or incomplete metathesis products such as $ThCl_2(O\text{-}2,6\text{-}t\text{-}Bu_2\text{-}4\text{-}Me\text{-}C_6H_2)_2$[15] and $ThCl(O\text{-}2,4,6\text{-}t\text{-}Bu_3C_6H_2)_3$.[15] In the latter case, even an excess of lithium aryloxide in refluxing THF failed to provide the homoleptic thorium complex of general formula $Th(OAr)_4$. Similar examples of incomplete metathesis have been observed by Rothwell and co-workers in the case of the group 4 metals. Thus the reaction of MCl_4 (M = Zr, Hf) with 4 equiv of $LiO\text{-}2,6\text{-}t\text{-}Bu_2C_6H_3$ yielded only the tris(aryloxide) species $MCl(O\text{-}2,6\text{-}t\text{-}Bu_2C_6H_3)_3$.[21]

However, following the methodology described earlier,[22] we find that the metathesis reaction of thorium tetraiodide or tetrabromide, $ThX_4(THF)_4$[23] (X = I, Br), with potassium aryloxide salts at room temperature results in complete metathesis, even in the case of the sterically-demanding 2,6-di-*tert*-butylphenoxide ligand, and allows the convenient and facile preparation of a series of thorium aryloxide complexes and their Lewis base adducts.

The reaction of $ThI_4(THF)_4$ with 4 equiv of potassium 2,6-di-*tert*-butylphenoxide in THF solution results in the formation of $Th(O\text{-}2,6\text{-}t\text{-}Bu_2C_6H_3)_4$ (**9**), in ca. 90% isolated yield as outlined in eq 5. In these reactions, the formation of relatively THF-

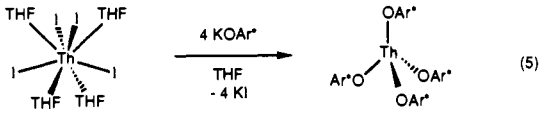

(5)

Ar* = 2,6-t-Bu2C6H3 (9)

insoluble KI may act as a driving force; thus we observe complete metathesis of iodide ligands and no formation of salt (or "double alkoxide") complexes. It is noteworthy that while this reaction is conducted in THF solution, the experimental workup procedures yield **9** as a base-free complex, presumably due to the steric demands of the bulky 2,6-di-*tert*-butylphenoxide ligand.

For less sterically-demanding aryloxide ligands, the metathesis reaction of $ThI_4(THF)_4$ or $ThBr_4(THF)_4$[23] with 4 equiv of $KO\text{-}2,6\text{-}R_2C_6H_3$ (R = Me, *i*-Pr) in THF solution results in the formation of the bis(THF) adducts $Th(O\text{-}2,6\text{-}R_2C_6H_3)_4(THF)_2$ [R = Me (**13**), *i*-Pr (**14**)] in ca. 60–70% yield according to eq 6. The

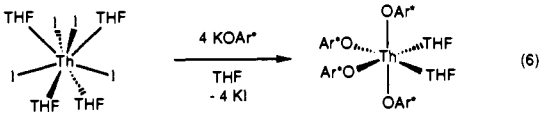

(6)

Ar* = 2,6-Me2C6H3 (13), 2,6-i-Pr2C6H3 (14)

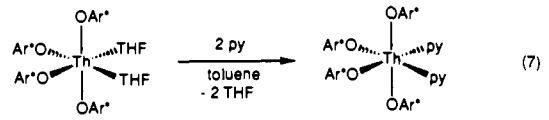

(7)

Ar* = 2,6-Me2C6H3 (15)

THF adducts readily exchange with other Lewis bases such as pyridine to give $Th(O\text{-}2,6\text{-}Me_2C_6H_3)_4(py)_2$ (**15**), as outlined in eq 7. The THF ligands of **13** and **14** are presumed to occupy cis positions, on the basis of the X-ray structural results obtained for the bis(pyridine) adduct **15** (vide infra). It is interesting to note at this point that Lappert and co-workers reported the metathesis reaction of uranium tetrachloride with $LiO\text{-}2,6\text{-}i\text{-}Pr_2C_6H_3$ in THF and obtained the *base-free* complex $U(O\text{-}2,6\text{-}i\text{-}Pr_2C_6H_3)_4$.[4] This may be a reflection of the slightly greater size of the thorium metal center compared to that of uranium.[24] We also note that Andersen has isolated the related tetraphenoxide phosphine adducts of formula $An(OPh)_4(dmpe)_2$ [An = U, Th; dmpe = 1,2-bis(dimethylphosphino)ethane] and has structurally characterized the uranium complex.[25]

Mechanistic Considerations. The first protonation step in the alcoholysis of the metallacycle $\{[(Me_3Si)_2N]_2An(CH_2SiMe_2NSiMe_3)\}$ [An = Th (**1**), U (**2**)] generates a mono(aryloxide) product $An(OAr^*)[N(SiMe_3)_2]_3$ consistent with protonation of the metal–carbon bond as indicated in eq 1. However, it is plausible that an amido An–N bond is protonated instead to produce free $HN(SiMe_3)_2$ and a new intermediate metallacycle of formula $(Ar^*O)[(Me_3Si)_2N]An(CH_2SiMe_2NSiMe_3)$. The free amine would then have to backreact with the new metallacycle and protonate the An–C bond in order to obtain the observed $An(OAr^*)[N(SiMe_3)_2]_3$ product. Such a scenario may be ruled out, however, due to the fact that when the mono(aryloxide) $An(O\text{-}2,6\text{-}t\text{-}Bu_2C_6H_3)[N(SiMe_3)_2]_3$ is heated (sealed NMR tube; An = U, ≥60 °C, C_6D_6; An = Th, ≥90 °C, $CD_3C_6D_5$), $HN(SiMe_3)_2$ is liberated and the new metallacycle $(2,6\text{-}t\text{-}Bu_2C_6H_3O)[(Me_3Si)_2N]An(CH_2SiMe_2NSiMe_3)$ [An = U (**16**), Th (**17**)] is formed as indicated in eq 8. Observation of the

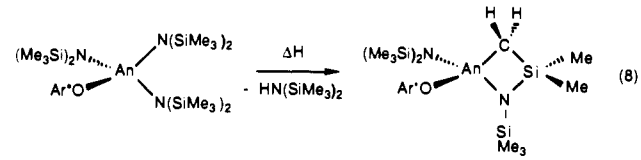

(8)

Ar* = 2,6-t-Bu2C6H3; An = U, (16); An = Th, (17)

reaction mixture by ^1H NMR reveals that the back reaction between free silylamine and the new metallacycle (**16** or **17**), to regenerate $An(O\text{-}2,6\text{-}t\text{-}Bu_2C_6H_3)[N(SiMe_3)_2]_3$, is *not* observed, either at room temperature or at elevated temperatures.

The reaction between the thorium mono(aryloxide) species $Th(O\text{-}2,6\text{-}t\text{-}Bu_2C_6H_3)[N(SiMe_3)_2]_3$ (**5**) and further equivalents of $HO\text{-}2,6\text{-}t\text{-}Bu_2C_6H_3$ is presumed to occur via stepwise protonation of amido Th–N bonds, to produce sequentially $Th(O\text{-}2,6\text{-}t\text{-}Bu_2C_6H_3)_2[N(SiMe_3)_2]_2$ (**7**) and $Th(O\text{-}2,6\text{-}t\text{-}Bu_2C_6H_3)_3[N(SiMe_3)_2]$ (**8**), which are readily isolated. The observation that this protonation sequence stops at the tris(aryloxide) complex **8** is probably an indication of steric congestion about the actinide metal center. Similar reactivity has been documented in the case of the group 4 amido species $M(NMe_2)_4$ (M = Ti, Zr), the reaction of which with excess $HO\text{-}2,6\text{-}t\text{-}Bu_2\text{-}4\text{-}MeC_6H_2$ at 120 °C yields only the bis(aryloxide) complex $M(NMe_2)_2(O\text{-}2,6\text{-}t\text{-}Bu_2\text{-}4\text{-}MeC_6H_2)_2$.[27]

Reducing the steric bulk of the substituents in the 2,6-positions on the phenol from *tert*-butyl to isopropyl produces a marked change in reactivity toward the metallacyclic species **1** and **2**, and we find that the homoleptic complexes $An(O\text{-}2,6\text{-}i\text{-}Pr_2C_6H_3)_4$ (An = Th, U) are both readily obtained after only several hours in refluxing toluene. This marked difference in reactivity may be compared to results obtained by Rothwell and co-workers for the alcoholysis of tetraalkyl zirconium species. Thus the reaction of $Zr(CH_2Ph)_4$ with $HO\text{-}2,6\text{-}t\text{-}Bu_2C_6H_3$ proceeds only as far as the bis(aryloxide) complex $Zr(CH_2Ph)_2(O\text{-}2,6\text{-}t\text{-}Bu_2C_6H_3)_2$, whereas $Zr(CH_2SiMe_3)_4$ reacts cleanly with 4 equiv of the less bulky phenol $HO\text{-}2,6\text{-}i\text{-}Pr_2C_6H_3$ to produce homoleptic $Zr(O\text{-}2,6\text{-}i\text{-}Pr_2C_6H_3)_4$.[26]

Solid-State and Molecular Structures. Four early actinide aryloxide compounds have been examined by single-crystal X-ray studies during this work: $U(O\text{-}2,6\text{-}t\text{-}Bu_2C_6H_3)[N(SiMe_3)_2]_3$ (**3**), $Th(O\text{-}2,6\text{-}t\text{-}Bu_2C_6H_3)_4$ (**9**), $U(O\text{-}2,6\text{-}t\text{-}Bu_2C_6H_3)_4$ (**11**), and Th-

(20) Many examples of actinide double alkoxides exist; Cotton, F. A.; Marler, D. O.; Schwotzer, W. *Inorg. Chem.* **1984**, *23*, 4211. Stewart, J. L.; Andersen, R. A. *J. Chem. Soc., Chem. Commun.* **1987**, 1846. Jones, R. G.; Bindschadler, E.; Blume, D.; Karmas, G.; Martin, G. A., Jr.; Thirtle, J. R.; Gilman, H. *J. Am. Chem. Soc.* **1956**, *78*, 6027. Cuellar, E. A.; Miller, S. S.; Marks, T. J.; Weitz, E. *J. Am. Chem. Soc.* **1983**, *105*, 4580. Caulton, K. G.; Hubert-Pfalzgraf, L. G. *Chem. Rev.* **1990**, *90*, 969. Mehrotra, R. C.; Singh, A.; Tripathi, U. M. *Chem. Rev.* **1991**, *91*, 1287.

(21) Latesky, S. L.; Keddington, J.; McMullen, A. K.; Rothwell, I. P.; Huffman, J. C. *Inorg. Chem.* **1985**, *24*, 995.

(22) Clark, D. L.; Bott, S. G.; Vrtis, R. N.; Sattelberger, A. P. *Inorg. Chem.* **1989**, *28*, 1771.

(23) Clark, D. L.; Frankcom, T. M.; Miller, M. M.; Watkin, J. G. *Inorg. Chem.* **1992**, *31*, 1628.

(24) Shannon, R. D. *Acta Crystallogr. A* **1976**, *32*, 751.

(25) Edwards, P. G.; Andersen, R. A.; Zalkin, A. *J. Am. Chem. Soc.* **1981**, *103*, 7792.

Table I. Summary of Crystal Data[a]

	3	9	11	15
empirical form	$UC_{32}H_{75}N_3OSi_6$	$ThC_{56}H_{84}O_4$	$UC_{56}H_{84}O_4$	$ThC_{49}H_{54}N_2O_4$
color of cryst	orange-brown	colorless	dark amber	colorless
cryst dimen, mm	0.10 × 0.12 × 0.10	0.05 × 0.07 × 0.07	0.10 × 0.12 × 0.10	0.20 × 0.12 × 0.12
space group	$P2_12_12_1$	$I\bar{4}$	$I\bar{4}$	$P2_1/n$
cell dimen				
a, Å	11.257 (3)	14.082 (5)	14.066 (2)	14.724 (3)
b, Å	19.761 (6)	14.082 (5)	14.066 (2)	19.724 (3)
c, Å	19.589 (7)	13.468 (5)	13.404 (2)	15.456 (2)
β, deg				100.95 (1)
temp, °C	−155	−171	−145	−171
Z (molecules/cell)	4	2	2	4
volume, Å^3	4357.46	2670.75	2652.10	4407.01
D_{calc}, g cm^{-3}	1.409	1.317	1.327	1.458
λ (Mo Kα)	0.71069	0.71069	0.71069	0.71069
formula wt	924.51	1053.29	1059.31	976.03
absorption coefficient, cm^{-1}	37.189	29.192	29.397	26.299
2θ range, deg	6–45	6–45	6–60	6–45
measured reflections	6222	3265	6503	8481
unique intensities	3226	1609	2026	5742
obsd reflections ($F > 2.33\sigma(F)$)	2984	1609	2020	4178
$R(F)$	0.0430	0.037	0.0294	0.0441
$R_w(F)$	0.0399	0.037	0.0296	0.0456
goodness-of-fit	0.933	0.948	1.139	1.214

[a] **3** = U(*O*-2,6-*t*-$Bu_2C_6H_3$)[$N(SiMe_3)_2$]$_3$, **9** = Th(*O*-2,6-*t*-$Bu_2C_6H_3$)$_4$, **11** = U(*O*-2,6-*t*-$Bu_2C_6H_3$)$_4$, **15** = Th(*O*-2,6-$Me_2C_6H_3$)$_4$(py)$_2$.

Table II. Selected Bond Distances (Å) for the U(*O*-2,6-*t*-$Bu_2C_6H_3$)[$N(SiMe_3)_2$]$_3$ Molecule

U(1)–O(2)	2.145 (8)	Si(36)–C(37)	1.866 (18)
U(1)–N(17)	2.286 (11)	Si(36)–C(38)	1.883 (17)
U(1)–N(26)	2.285 (10)	Si(36)–C(39)	1.881 (16)
U(1)–N(35)	2.283 (10)	Si(36)–N(35)	1.741 (13)
Si(18)–N(17)	1.764 (12)	Si(40)–N(35)	1.759 (12)
Si(18)–C(19)	1.854 (15)	Si(40)–C(41)	1.890 (14)
Si(18)–C(20)	1.886 (17)	Si(40)–C(42)	1.862 (16)
Si(18)–C(21)	1.870 (13)	Si(40)–C(43)	1.856 (15)
Si(22)–N(17)	1.746 (13)	O(2)–C(3)	1.382 (15)
Si(22)–C(23)	1.866 (16)	Si(27)–C(30)	1.903 (17)
Si(22)–C(24)	1.882 (15)	Si(31)–N(26)	1.769 (11)
Si(22)–C(25)	1.867 (14)	Si(31)–C(32)	1.858 (16)
Si(27)–N(26)	1.741 (11)	Si(31)–C(33)	1.870 (16)
Si(27)–C(28)	1.883 (15)	Si(31)–C(34)	1.853 (17)
Si(27)–C(29)	1.863 (16)		

(*O*-2,6-$Me_2C_6H_3$)$_4$(py)$_2$ (**15**). In each case, the unit cell revealed discrete monomeric species. A summary of data collection and crystallographic parameters is given in Table I.

A. U(*O*-2,6-*t*-$Bu_2C_6H_3$)[$N(SiMe_3)_2$]$_3$ (3). Crystals of **3** suitable for X-ray diffraction were grown from concentrated THF solution at −40 °C. A ball and stick drawing giving the atom-numbering scheme used in the tables is given in Figure 1. Selected bond distances and bond angles are given in Tables II and III, respectively. U(*O*-2,6-*t*-$Bu_2C_6H_3$)[$N(SiMe_3)_2$]$_3$ (**3**) crystallizes in the orthorhombic space group $P2_12_12_1$. The central uranium atom is coordinated in a distorted tetrahedral fashion by the oxygen atom of the aryloxide ligand and the nitrogen atoms of the three silylamide ligands (Figure 1). In the solid state, the aryloxide ligand of **3** is oriented such that there are two different *tert*-butyl environments, one lying over a U–N bond and one bisecting the remaining two U–N bonds. The U–O distance of 2.145 (8) Å is similar to the average U–O bond lengths of 2.143 (4),[15] 2.17 (1),[25] and 2.17 (2) Å[14] observed in $(Et_2N)U(O\text{-}2,6\text{-}t\text{-}Bu_2C_6H_3)_3$, $U(OPh)_4(dmpe)_2$, and $[Li(THF)_4][U(O\text{-}2,6\text{-}i\text{-}Pr_2C_6H_3)_5]$, respectively. The U–O–C angle is 158.6 (8)°. The average U–N distance of 2.285 (11) Å in **3** is very close to those found previously for terminal, tetravalent U–N bond lengths in $[U(NEt_2)_4]_2$, $[U(MeNCH_2CH_2NMe)_2]_3$, $[U(MeNCH_2CH_2NMe)_2]_4$, $U(NPh_2)_4$, $HU[N(SiMe_3)_2]_3$, and $(Et_2N)U(O\text{-}2,6\text{-}t\text{-}Bu_2C_6H_3)_3$, which are 2.22,[28] 2.21,[29] 2.27,[30] 2.24,[31] 2.24,[32] and 2.16 Å,[15] respectively.

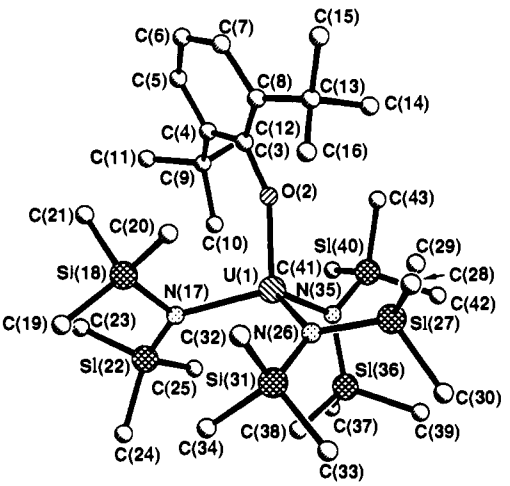

Figure 1. Ball and stick drawing of the solid-state molecular structure of U(*O*-2,6-*t*-$Bu_2C_6H_3$)[$N(SiMe_3)_2$]$_3$ (**3**).

Table III. Selected Bond Angles (deg) for the U(*O*-2,6-*t*-$Bu_2C_6H_3$)[$N(SiMe_3)_2$]$_3$ Molecule

O(2)–U(1)–N(17)	102.5 (4)	Si(36)–N(35)–Si(40)	115.3 (6)
O(2)–U(1)–N(26)	118.4 (4)	U(1)–N(35)–Si(40)	129.1 (6)
O(2)–U(1)–N(35)	103.4 (4)	U(1)–N(35)–Si(36)	115.5 (6)
N(17)–U(1)–N(26)	107.9 (4)	Si(27)–N(26)–Si(31)	114.6 (6)
N(17)–U(1)–N(35)	118.8 (4)	U(1)–N(26)–Si(31)	129.4 (6)
N(26)–U(1)–N(35)	106.5 (4)	U(1)–N(26)–Si(27)	116.0 (5)
N(17)–Si(18)–C(19)	113.3 (6)	Si(18)–N(17)–Si(22)	116.0 (6)
N(17)–Si(18)–C(20)	108.3 (6)	N(35)–Si(40)–C(42)	113.8 (6)
N(17)–Si(18)–C(21)	115.5 (6)	N(35)–Si(40)–C(41)	112.0 (6)
U(1)–N(17)–Si(22)	129.5 (6)	N(26)–Si(27)–C(28)	111.7 (7)
U(1)–N(17)–Si(18)	114.0 (6)	N(26)–Si(27)–C(29)	108.4 (6)
U(1)–O(2)–C(3)	158.6 (8)	N(26)–Si(27)–C(30)	114.1 (7)
N(17)–Si(22)–C(23)	113.5 (6)	N(35)–Si(36)–C(39)	115.5 (7)
N(17)–Si(22)–C(24)	112.1 (7)	N(35)–Si(36)–C(38)	107.8 (6)
N(17)–Si(22)–C(25)	111.4 (6)	N(35)–Si(36)–C(37)	112.7 (7)
N(35)–Si(40)–C(43)	114.4 (6)	N(26)–Si(31)–C(33)	114.4 (6)
N(26)–Si(31)–C(32)	113.0 (6)	N(26)–Si(31)–C(34)	112.5 (7)

B. An(*O*-2,6-*t*-$Bu_2C_6H_3$)$_4$ [An = Th (9), U (11)]. Homoleptic four-coordinate actinide complexes are quite rare, with the only

(26) Latesky, S. L.; McMullen, A. K.; Niccolai, G. P.; Rothwell, I. P.; Huffman, J. C. *Organometallics* **1985**, *4*, 902.
(27) Duff, A. W.; Kamarudin, R. A.; Lappert, M. F.; Norton, R. J. *J. Chem. Soc., Dalton Trans.* **1986**, 489.
(28) Reynolds, J. G.; Zalkin, A.; Templeton, D. H.; Edelstein, N. M.; Templeton, L. K. *Inorg. Chem.* **1976**, *15*, 2498.
(29) Reynolds, J. G.; Zalkin, A.; Templeton, D. H.; Edelstein, N. M. *Inorg. Chem.* **1977**, *16*, 599.

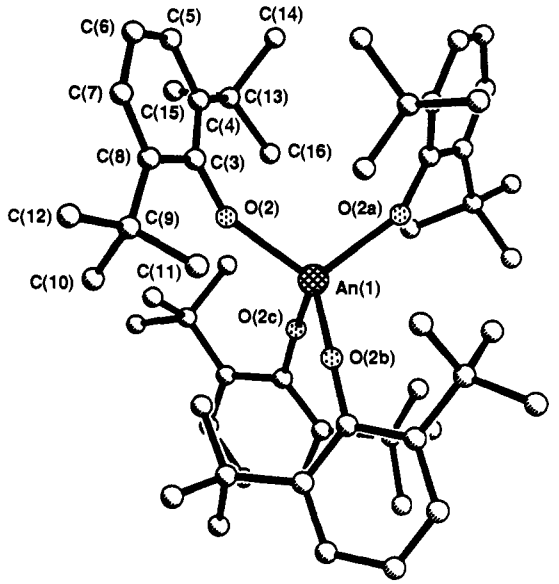

Figure 2. Ball and stick drawing of the solid-state molecular structure of An(*O*-2,6-*t*-$Bu_2C_6H_3)_4$ viewed perpendicular to the S_4 axis, emphasizing S_4 symmetry.

Table IV. Selected Bond Distances (Å) for An(*O*-2,6-*t*-$Bu_2C_6H_3)_4$ Molecules

	An = uranium	An = thorium
An(1)–O(2)	2.135 (4)	2.189 (6)
O(2)–C(3)	1.344 (14)	1.341 (19)
C(3)–C(4)	1.462 (16)	1.394 (22)
C(3)–C(8)	1.413 (13)	1.464 (20)
C(4)–C(5)	1.405 (9)	1.382 (12)
C(4)–C(13)	1.553 (9)	1.570 (12)
C(5)–C(6)	1.376 (10)	1.402 (13)
C(6)–C(7)	1.384 (11)	1.369 (14)
C(7)–C(8)	1.376 (10)	1.380 (13)
C(8)–C(9)	1.535 (9)	1.534 (12)

Table V. Selected Bond Angles (deg) for An(*O*-2,6-*t*-$Bu_2C_6H_3)_4$ Molecules

	An = uranium	An = thorium
O(2)–An(1)–O(2b)	110.23 (12)	110.46 (15)
O(2)–An(1)–O(2a)	107.96 (23)	107.5 (3)
An(1)–O(2)–C(3)	154.0 (6)	153.5 (10)
O(2)–C(3)–C(4)	119.9 (9)	124.5 (14)
C(4)–C(3)–C(8)	118.1 (10)	118.2 (14)
C(3)–C(4)–C(5)	117.2 (7)	120.1 (10)
C(3)–C(4)–C(13)	128.2 (7)	124.6 (10)
C(5)–C(4)–C(13)	114.6 (6)	115.3 (8)
C(4)–C(5)–C(6)	123.0 (6)	121.4 (8)
C(5)–C(6)–C(7)	117.9 (6)	118.7 (8)
C(6)–C(7)–C(8)	123.1 (6)	122.6 (8)
C(3)–C(8)–C(7)	119.5 (8)	118.1 (11)
C(3)–C(8)–C(9)	120.6 (8)	122.3 (10)
C(7)–C(8)–C(9)	119.9 (5)	119.6 (7)
C(4)–C(13)–C(15)	106.6 (6)	107.9 (8)
C(4)–C(13)–C(16)	118.1 (8)	119.8 (10)
C(14)–C(13)–C(15)	110.8 (8)	109.4 (10)

other structurally characterized example being $U[N(C_6H_5)_2]_4$.[31] This study provides the first structural characterization of a four-coordinate, homoleptic $Th(OAr)_4$ compound. Single-crystal X-ray structures have been determined for the two complexes An(*O*-2,6-*t*-$Bu_2C_6H_3)_4$ [An = Th (**9**), U (**11**)]. Crystals of suitable quality were grown by slow evaporation of a toluene solution (**9**)

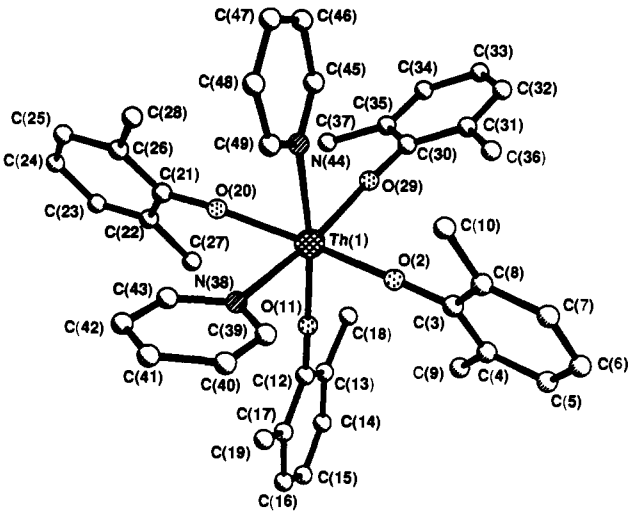

Figure 3. Ball and stick drawing of the solid-state molecular structure of Th(*O*-2,6-$Me_2C_6H_3)_4(py)_2$ emphasizing the cis pseudo-octahedral symmetry.

Table VI. Selected Bond Distances (Å) for Th(*O*-2,6-$Me_2C_6H_3)_4(py)_2{\cdot}C_6H_5Me$

Th(1)–O(2)	2.211 (6)	O(11)–C(12)	1.338 (12)
Th(1)–O(11)	2.188 (6)	O(20)–C(21)	1.355 (12)
Th(1)–O(20)	2.206 (6)	O(29)–C(30)	1.354 (12)
Th(1)–O(29)	2.183 (6)	N(38)–C(39)	1.353 (13)
Th(1)–N(38)	2.662 (8)	N(38)–C(43)	1.343 (14)
Th(1)–N(44)	2.696 (8)	N(44)–C(45)	1.347 (12)
O(2)–C(3)	1.343 (12)	N(44)–C(49)	1.334 (13)

Table VII. Selected Bond Angles (deg) for Th(*O*-2,6-$Me_2C_6H_3)_4(py)_2{\cdot}C_6H_5Me$

O(2)–Th(1)–O(11)	94.37 (24)	O(20)–Th(1)–N(44)	81.96 (24)
O(2)–Th(1)–O(20)	162.53 (26)	O(29)–Th(1)–N(38)	163.92 (24)
O(2)–Th(1)–O(29)	93.76 (23)	O(29)–Th(1)–N(44)	85.84 (24)
O(2)–Th(1)–N(38)	82.21 (25)	N(38)–Th(1)–N(44)	78.40 (24)
O(2)–Th(1)–N(44)	86.56 (24)	Th(1)–O(2)–C(3)	169.1 (7)
O(11)–Th(1)–O(20)	94.99 (24)	Th(1)–O(11)–C(12)	175.8 (6)
O(11)–Th(1)–O(29)	102.90 (23)	Th(1)–O(20)–C(21)	172.0 (6)
O(11)–Th(1)–N(38)	92.95 (24)	Th(1)–O(29)–C(30)	176.2 (6)
O(11)–Th(1)–N(44)	171.11 (24)	Th(1)–N(38)–C(39)	120.9 (7)
O(20)–Th(1)–O(29)	98.47 (24)	Th(1)–N(38)–C(43)	122.2 (7)
O(20)–Th(1)–N(38)	82.61 (24)		

or by cooling of a concentrated hexane solution to −40 °C (**11**). The compounds are isostructural and possess crystallographic $\bar{4}$ (S_4) symmetry, giving only one unique aryloxide ligand. A view of the basic structural motif emphasizing S_4 symmetry is shown in Figure 2. Selected bond distances and bond angles are given in Tables IV and V, respectively. Each set of four An–O bond lengths is identical [2.189 (6) Å, Th, and 2.135 (4) Å, U], and the O–An–O angles are of two types, four of 110.46 (15)° for An = Th [110.2 (1), An = U] and two of 107.5 (3)° for An = Th [108.0 (2), An = U]. The latter angles are those bisected by the C_2 (S_4) axis and correspond to a slight flattening of the central AnO_4 core from T_d to D_{2d} symmetry. The Th–O–C angle of 153.5 (10)° is essentially identical to the U–O–C angle of 154.0 (6)°. The U–O bond distance of 2.135 (4) Å in U(*O*-2,6-*t*-$Bu_2C_6H_3)_4$ (**11**) may be compared to those of 2.143 (4),[15] 2.17 (1),[27] 2.17 (2),[14] and 2.132 (8)[33] observed in $(Et_2N)U$(*O*-2,6-*t*-$Bu_2C_6H_3)_3$, $U(OPh)_4(dmpe)_2$, $[Li(THF)_4][U$(*O*-2,6-*i*-$Pr_2C_6H_3)_5]$, and $[U$(*O*-2,6-*i*-$Pr_2C_6H_3)_3]_2$, respectively. The Th–O bond length of 2.189 (6) Å is similar in magnitude to the Th–O distance of 2.190 (9) Å observed for the 2,6-di-*tert*-butylphenoxide ligand in Th(*O*-2,6-*t*-$Bu_2C_6H_3)_2(CH_2$-py-6-$Me)_2$[34] and 2.154 (8) Å observed for

(30) Reynolds, J. G.; Zalkin, A.; Templeton, D. H.; Edelstein, N. M. *Inorg. Chem.* **1977**, *16*, 1858.
(31) Reynolds, J. G.; Zalkin, A.; Templeton, D. H.; Edelstein, N. M. *Inorg. Chem.* **1977**, *16*, 1090.
(32) Andersen, R. A.; Zalkin, A.; Templeton, D. H. *Inorg. Chem.* **1981**, *20*, 622.
(33) Van Der Sluys, W. G.; Burns, C. J.; Huffman, J. C.; Sattelberger, A. P. *J. Am. Chem. Soc.* **1988**, *110*, 5924.
(34) Beshouri, S. M.; Fanwick, P. E.; Rothwell, I. P.; Huffman, J. C. *Organometallics* **1987**, *6*, 2498.

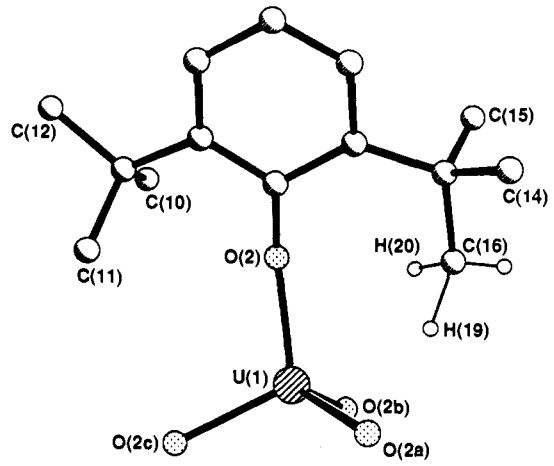

Figure 4. Ball and stick drawing of the solid-state molecular structure of U(*O*-2,6-*t*-$Bu_2C_6H_3)_4$ emphasizing the coordination geometry of the *O*-2,6-*t*-$Bu_2C_6H_3$ ligand.

the 2-butene-2,3-diolate ligand in the X-ray structure of $[(\eta^5\text{-}C_5Me_5)_2Th(\mu\text{-}O_2C_2Me_2)]_2$.[35]

C. Th(*O*-2,6-$Me_2C_6H_3)_4(py)_2$ (15). Crystals of **15** suitable for X-ray diffraction were grown from a concentrated toluene solution at −40 °C. A view of the molecule, giving the atom-numbering scheme used in the tables is shown in Figure 3. Selected bond distances and bond angles are given in Tables VI and VII, respectively. The compound crystallizes in the monoclinic space group $P2_{1/n}$ and exhibits a pseudo-octahedral geometry about the central thorium atom with the two pyridine ligands occupying cis positions (Figure 3); average Th–N and Th–O distances are 2.679 (8) and 2.198 (6) Å, respectively. These Th–O distances are in the same range as seen in the solid-state structure of Th(*O*-2,6-*t*-$Bu_2C_6H_3)_4$ (**9**) and Th(*O*-2,6-*t*-$Bu_2C_6H_3)_2(CH_2\text{-py-6-Me})_2$.[34] The Th–N distance is comparable to that of 2.61 (1) Å observed for the 2-(6-methylpyridyl)methyl ligand of Th(*O*-2,6-*t*-$Bu_2C_6H_3)_2(CH_2\text{-py-6-Me})_2$.[34] The four aryloxide ligands are found to display relatively large Th–O–C angles ranging from 170.6 to 176.0°.

Coordination Properties of the 2,6-Di-*tert*-butylphenoxide Ligand Bound to Actinide Metals. The coordination of the 2,6-di-*tert*-butylphenoxide ligand to actinide metals displays properties similar to that described for early transition metals; short M–O distances and large M–O–C(ipso) angles.[36] However, for all three structures reported here, the conformations of the two *tert*-butyl constituents are asymmetric with respect to their orientation toward the actinide metal center, as shown in Figure 4 for **11**. For one of the *tert*-butyl groups, centered on C(9), a "normal" conformation is found such that the distance between the actinide metal atom and its methyl groups is maximized as one might expect for such a bulky substituent. However, the other *tert*-butyl group has adopted the exact opposite conformation, with a unique methyl group pointed directly toward the actinide metal center. For both **9** and **11**, low-temperature X-ray diffraction data were collected. For **9**, a difference Fourier located most of the hydrogen atoms, but when attempts were made to refine their positions, several were poorly behaved and failed to converge. However, for **11**, all of the hydrogen atoms were refined. A ball and stick view of the 2,6-di-*tert*-butylphenoxide ligand in **11** is shown in Figure 4 emphasizing the actinide metal coordination sphere and indicating the refined hydrogen atoms of the unique methyl group closest to the metal center. This unusual conformation has been observed in only a few other structures of early d-block transition metal complexes and has been discussed in detail by Rothwell.[36] None of the C–H bonds are oriented directly toward the U center in a planar M–H–C–C fashion. Two hydrogen atoms, H(19) and

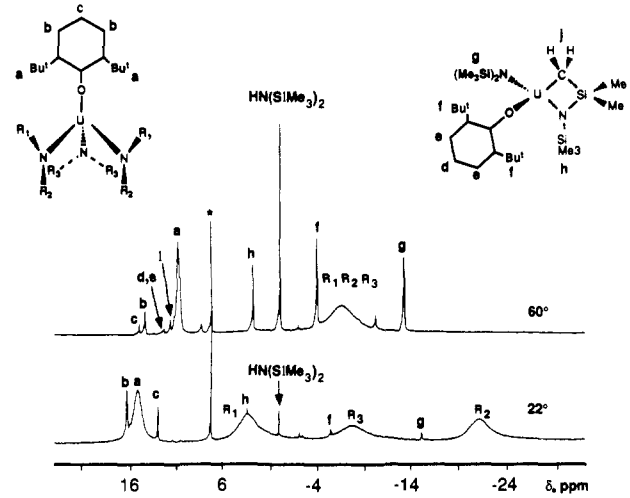

Figure 5. (Bottom) ^1H NMR spectrum of U(*O*-2,6-*t*-$Bu_2C_6H_3$)[N-$(SiMe_3)_2]_3$ at 22 °C in C_6D_6. (Top) ^1H NMR spectrum of U(*O*-2,6-*t*-$Bu_2C_6H_3$)[$N(SiMe_3)_2]_3$ at 60 °C in C_6D_6. NMR peak assignments of U(*O*-2,6-*t*-$Bu_2C_6H_3$)[$N(SiMe_3)_2]_3$ and its thermolysis product, [2,6-*t*-$Bu_2C_6H_3O$][$(Me_3Si)_2N$]UN($SiMe_3$)$SiMe_2CH_2$ are as indicated in the drawings shown above the figure. The diastereotopic methylene protons, j, appear at δ −151.2 and −191.9 ppm. The ^1H impurity of the C_6D_6 solvent is marked by an asterisk.

H(20), have close U--H contacts of 2.52 and 2.89 Å, respectively. Although these U--H contacts are close, we have observed no spectroscopic evidence in support of agostic interactions,[37] nor have we observed any thermal cyclometallation chemistry in which these C–H bonds are activated or cleaved, as has been observed in early transition metal complexes with this ligand.[38]

Spectroscopic Studies. A. Solution ^1H NMR Studies. At room temperature the ^1H NMR spectrum of U(*O*-2,6-*t*-$Bu_2C_6H_3$)[N-$(SiMe_3)_2]_3$ (**3**) in C_6D_6 consists of four broad signals of equal integral intensity centered at 15.0, 3.5, −8.0, and −22.1 ppm, together with the signals of the ortho and para protons of the aryloxide ligand (Figure 5). Upon raising the temperature to +60 °C, the three signals assigned to the silylamide ligands coalesce into a single resonance centered at −6.5 ppm. The fourth signal, now centered at 10.5 ppm, sharpened somewhat and is assigned to the *tert*-butyl resonance of the aryloxide ligand. It should be noted that at this temperature the compound slowly decomposes to the new metallacyclic compound (2,6-*t*-$Bu_2C_6H_3O$)[$(Me_3Si)_2N$]U($CH_2SiMe_2NSiMe_3$) (**16**) along with the liberation of $HN(SiMe_3)_2$ (vide supra). The NMR assignments for **16** are listed in Figure 5. Below room temperature the three silylamide signals of **3** sharpen, and at −70 °C the *tert*-butyl resonance becomes complex, indicating the onset of restricted rotation within the *tert*-butyl groups.

The low-temperature limiting spectrum of **3** may be rationalized on the basis of structures possessing a mirror plane of symmetry. Two plausible structures are shown in A and B, which represent

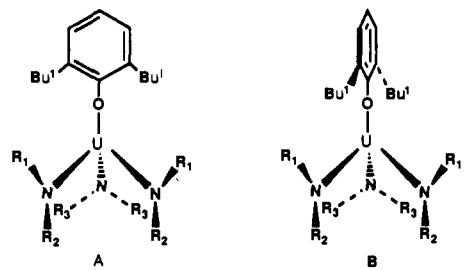

schematic views of **3** looking down the mirror plane containing C(ipso)–O–U–N. Note that either A or B would give rise to three

(35) Manriquez, J. M.; Fagan, P. J.; Marks, T. J.; Day, C. S.; Day, V. W. *J. Am. Chem. Soc.* **1978**, *100*, 7112.
(36) Fanwick, P. W.; Ogilvy, A. E.; Rothwell, I. P. *Organometallics* **1987**, *6*, 73.
(37) Brookhart, M.; Green, M. L. H.; Wong, L. L. *Prog. Inorg. Chem.* **1988**, *36*, 1.
(38) Rothwell, I. P. *Polyhedron* **1985**, *4*, 177 and references therein.

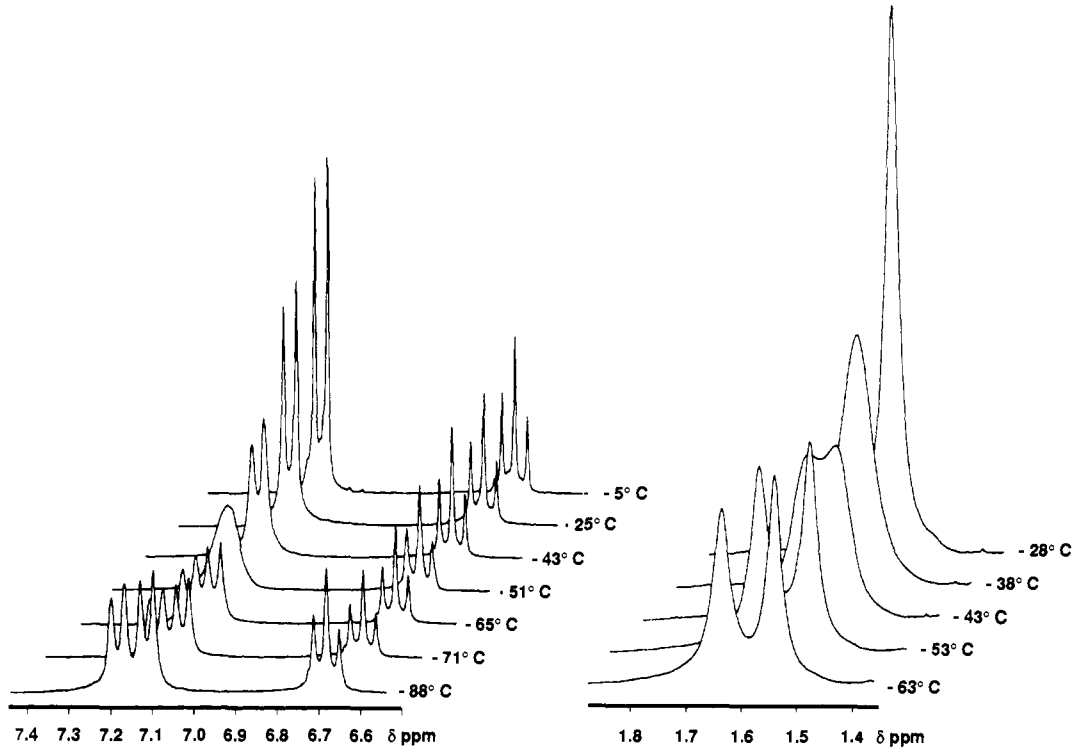

Figure 6. Variable-temperature ^{1}H NMR behavior of Th(*O*-2,6-*t*-$Bu_2C_6H_3)_4$ showing the behavior of aromatic meta and para protons on the left and *t*-Bu protons on the right.

types of silylamide ligands in a 1:1:1 ratio as indicated (R_1, R_2, R_3) in the drawing. Restricted rotation about the U–N bonds of the two silylamide ligands related by the plane of symmetry would result in two different $SiMe_3$ signals for groups proximal and distal to the aryloxide ligand labeled as R_1 and R_2 in the schematic drawing. The same plane of symmetry renders equivalent the $SiMe_3$ groups of the third silylamide ligand (R_3). Structure B is consistent with the observed ^{1}H NMR data only if there is rapid rotation about the U–O and/or the O–C bond of the phenoxide ligand.

The structure illustrated in B most closely approximates that observed in the solid-state structure of **3**. Structures A and B are both consistent with the room temperature ^{1}H NMR spectra (Figure 5), assuming rapid rotation about the U–O or O–C bond in B and restricted rotation about the U–N bonds. At elevated temperatures (+60 °C), rapid rotation about the U–N bonds renders equivalent all $SiMe_3$ groups, producing the observed coalescence of ^{1}H NMR resonances. At room temperature, the analogous monoaryloxide thorium complex Th(*O*-2,6-*t*-$Bu_2C_6H_3)[N(SiMe_3)_2]_3$ (**5**) shows a single silylamide and a single *tert*-butyl environment in a 3:1 ratio, similar to the high-temperature spectral features seen in the uranium analogue. This may be a further reflection of the greater size of the Th(IV) metal center compared with that of U(IV).[24]

^{1}H NMR spectra of the homoleptic An(*O*-2,6-*t*-$Bu_2C_6H_3)_4$ [An = Th (**9**), U (**11**)] complexes reveal a single 2,6-di-*tert*-butylphenoxide environment at ambient temperature. Low-temperature (185 K) solution ^{1}H NMR spectra (Figure 6; An = Th), however, reveal chemically-inequivalent *tert*-butyl and meta proton resonances yet a single para proton resonance for the 2,6-di-*tert*-butylphenoxide ligand. This is indicative of S_4 symmetry in solution at low temperature in agreement with expectations based on the solid-state structures. Upon raising the temperature, the para proton remains a sharp triplet (Figure 6), while the *tert*-butyl and meta proton (doublet) resonances coalesce into single sharp resonances with average chemical shift values consistent with rapid rotation about An–O or O–C bonds. The activation energy $\Delta G^{\ddagger}$ for the rotational process is 11.6 (1) kcal for **9**. Similar behavior has been observed in the low-temperature ^{1}H NMR spectra of the tris(aryloxide) species HfCl(*O*-2,6-*t*-$Bu_2C_6H_3)_3$ and TiI(*O*-2,6-*t*-$Bu_2C_6H_3)_3$.[21]

The room temperature ^{1}H NMR spectra of the Lewis base adducts $Th(OAr)_4L_2$ (**13–15**) show only one type of aryloxide and Lewis base environment in solution at room temperature. Variable-temperature studies reveal a broadening of these resonances at lower temperatures, but we are unable to reach a limiting spectrum, even at −90 °C due to rapid scrambling of ligands in these systems. In the room temperature ^{1}H NMR spectrum of Th(*O*-4-*t*-$BuC_6H_4)_4(py)_3$ (**10**), only a single aryloxide environment is observed, presumably as a result of a rapid fluxional process within this seven-coordinate complex. At low temperature (185 K) in $C_6D_5CD_3$, the *tert*-butyl resonance is seen to broaden slightly but no static structure could be frozen out. Since we were unable to obtain X-ray quality crystals, the question of the stereochemistry of **10** remains unresolved.

B. Electronic Absorption Spectra. Four-coordinate actinide complexes are quite rare, as are complexes with T_d symmetry. The only actinide complexes with T_d symmetry which have had their spectra analyzed in any detail are $U(BH_4)_4$ and $U(BH_3C-H_3)_4$, and in both cases the uranium atom is 12-coordinate.[39] The majority of the other known actinide alkoxide complexes tend to be six-coordinate, with pseudo-octahedral symmetry about the actinide metal center.[3,4] Thus the homoleptic U(*O*-2,6-*t*-$Bu_2C_6H_3)_4$ system presents a unique opportunity to analyze the electronic structure of a four-coordinate, nearly T_d, $5f^2$ system.

The electronic absorption spectra of U(IV) compounds **3** and **11** in THF solution are shown in Figure 7. The rising absorption edges in the high-energy region near 20000 cm^{-1} are due to charge-transfer transitions, probably of the ligand-to-metal (LMCT) type. All of the bands to lower energy are assigned to U-centered transitions between energy levels of the $5f^2$ configuration. The general appearance of these bands matches what is observed for U(IV) doped into crystalline matrices such as $ThCl_4$ and $ThBr_4$,[40] as well as for the aquo U^{4+} ion stabilized in acid solution.[41] The energy levels indicated by the observed transitions correlate well with the free-ion $5f^2$ energy levels.[42]

(39) Rajnak, K.; Gamp, E.; Shinomoto, R.; Edelstein, N. M. *J. Chem. Phys.* **1984**, *80*, 5942.
(40) Krupa, J. C. *Inorg. Chim. Acta* **1987**, *139*, 223.
(41) Carnall, W. T.; Crosswhite, H. M. In *The Chemistry of the Actinide Elements*; Katz, J. J., Seaborg, G. T., Morss, L. R., Eds.; Chapman and Hall: New York, 1986; p 1265.

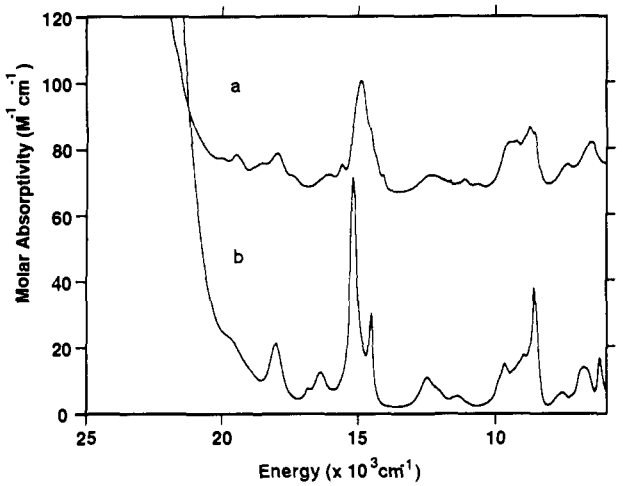

Figure 7. Electronic absorption spectra of (a) U(*O*-2,6-*t*-$Bu_2C_6H_3$)[N($SiMe_3$)$_2$]$_3$ (**3**) and (b) U(*O*-2,6-*t*-$Bu_2C_6H_3$)$_4$ (**11**) recorded in THF solution at 22 °C.

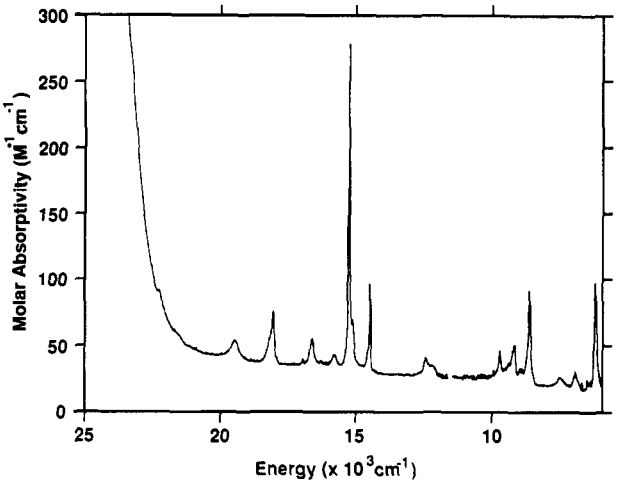

Figure 8. Electronic absorption spectrum of U(*O*-2,6-*t*-$Bu_2C_6H_3$)$_4$ (**11**) recorded in methylcyclohexane glass at −78 °C.

The $5f^2$ configuration gives rise to 13 states in the free U^{4+} ion. In a low-symmetry ligand field, degeneracies within the free-ion states are lifted, and up to 91 energy levels may result. In T_d symmetry many degeneracies are preserved in the complex, and the $5f^2$ configuration produces 40 energy levels. Of these, 33 are expected to fall within the energy range above the ground state which is sampled by the spectra in Figure 7. Transitions from the ground state to excited levels will be relatively weak because the parity-forbidden nature of the transitions in the isotropic free ion carries over to some extent to the anisotropic complex. They are allowed because the ligand field, which lacks a center of inversion, induces mixing with other atomic configurations of the opposite parity (5f6d, etc.). The spectra reflect these influences in that the f–f transitions between 5000 and 20 000 cm^{-1} are considerably weaker than the LMCT bands, having maximum molar extinction coefficients of around 40 M^{-1} cm^{-1}, but are stronger than the analogous bands in lanthanide complexes by about a factor of 10 due to the greater interaction of the 5f orbitals with the ligands.

The relative simplicity of the spectrum of **11** shown in Figure 7 is a particular unique characteristic of what we expect to see from a tetrahedral complex. High symmetry reduces the number of energy levels and introduces selection rules which weaken or forbid some transitions. Since the lack of a center of inversion makes vibronic interactions unnecessary to break the parity selection rule for electric dipole transitions, electronic origin bands are expected to be strong relative to vibronic side bands. This results in a much simpler spectrum in the T_d case than in the equally high symmetry and more common octahedral case where electric dipole transitions remain forbidden without the involvment of some symmetry-breaking vibration. The sharpness of the transitions is emphasized in the low-temperature spectrum shown in Figure 8. We expect to exploit this property in quantitative modeling of the spectra of **11** in future work.

While the spectra in Figure 7 are similar, they do show differences which are manifestations of the effects of the ligands on the electronic structure of uranium. While both **3** and **11** are four-coordinate, the ligands are not equivalent in **3**. The spectra of **3** are better considered as resulting from a complex with C_{3v} symmetry about the central uranium atom. Under these conditions there will be approximately 50 energy levels in the region sampled by the spectra in Figure 7, which is 50% more than there were in the case of **11**. The expected increase in complexity of the spectra is evident in Figure 7, although it is difficult to quantify because the peaks in the spectra of **3** are not well resolved.

C. Electrochemistry. The cyclic voltammetric behavior of U(*O*-2,6-*t*-$Bu_2C_6H_3$)$_4$ (**11**) was examined in THF/0.1 M tetrabutylammonium tetrafluoroborate solution. The system is characterized by an irreversible reduction wave near the cathodic solvent limit and an irreversible oxidation wave at approximately the same potential as that of ferrocene, which was used as an internal standard. This irreversible behavior persisted for both waves even at scan rates as high as 50 V s^{-1}.

Controlled potential electrolysis at a potential just positive of the oxidation wave proceeds with the consumption of exactly 2 equiv of electrons per mole of compound, indicating oxidation of uranium to the +6 oxidation state and removal of the two electrons which are populating the nearly degenerate 5f orbitals. A voltammogram of the solution following electrolysis shows several small irreversible reduction waves. Apparently the oxidized compound reacts with the solvent system to generate several different products. Similar results are obtained with controlled potential electrolysis at the reduction wave. A Coulometric analysis of this reduction gives a number slightly greater than 1 equiv of electrons per mole of compound, but an accurate analysis is precluded by the proximity of the wave to the solvent limit. Most likely the electrolysis proceeds with the reduction of uranium to the 3+ state and subsequent decomposition of this complex. Further evidence for this mechanism is provided by the presence of several new irreversible oxidation waves that appear in the voltammogram following electrolysis.

Concluding Remarks

A range of new four-, six-, and seven-coordinate actinide aryloxide complexes have been prepared using either metathesis reactions of actinide tetrahalides or the alcoholysis of an actinide amido complex. The preparation of Th(*O*-2,6-*t*-$Bu_2C_6H_3$)$_4$ from $ThI_4(THF)_4$ and potassium aryloxide has demonstrated the enhanced synthetic utility of these reagents over the more commonly used metal tetrachloride and lithium alkoxide combination. The actinide metallacycle [{$(Me_3Si)_2N$}$_2$An($CH_2SiMe_2NSiMe_3$)] (An = Th, U) has been shown to react with 4 equiv of less bulky phenols HO-2,6-$R_2C_6H_3$ (R = H, Me, *i*-Pr) to produce tetrakis(aryloxide) complexes, while in the case of thorium, the reaction with >4 equiv of the sterically-demanding HO-2,6-*t*-$Bu_2C_6H_3$ even at 130 °C leads only to the tris(aryloxide) species Th(*O*-2,6-*t*-$Bu_2C_6H_3$)$_3$[N($SiMe_3$)$_2$]. The reaction between the mono(aryloxide) species An(*O*-2,6-*t*-$Bu_2C_6H_3$)[N($SiMe_3$)$_2$]$_3$ and further equivalents of HO-2,6-*t*-$Bu_2C_6H_3$ is presumed to occur via stepwise protonation of An–N bonds, to produce sequentially An(*O*-2,6-*t*-$Bu_2C_6H_3$)$_2$[N($SiMe_3$)$_2$]$_2$ and An(*O*-2,6-*t*-$Bu_2C_6H_3$)$_3$[N($SiMe_3$)$_2$], which are readily isolated for An = Th. The observation that this protonation stops at the tris(aryloxide) complex for thorium could be taken as an indication of steric congestion about the metal center. There is, however, an obvious dilemma

(42) Wyart, J. F.; Kaufman, V.; Sugar, J. *Phys. Scr.* **1980**, *22*, 389. Van Deurzen, C. H. H.; Rajnak, K.; Conway, J. G. *J. Opt. Soc. Am.* **1984**, *B1*, 45.

(43) Chisholm, M. H. *Polyhedron* **1983**, *2*, 681. Chisholm, M. H.; Clark, D. L. *Comments Inorg. Chem.* **1987**, *6*, 23.

with this explanation. As noted earlier, the ionic radius of uranium is smaller than that of thorium. If steric arguments are invoked to explain why the thorium protonolysis reactions fail to provide $Th(OAr^*)_4$, then how is it possible that the uranium protonolysis reactions, involving a necessarily more congested metal center, yield $U(OAr^*)_4$ as the final product. One possible explanation is oxidative addition of $HOAr^*$ to $U(OAr^*)_3[N(SiMe_3)_2]$[44] followed by reductive elimination of $HN(SiMe_3)_2$. Such a sequence of reactions is impossible in the case of thorium because thorium(IV) is the ultimate oxidation state.

There is structural evidence in support of π-bonding interactions in the actinide alkoxide complexes reported here. For all four structures, the alkoxide interactions show relatively short An–O bonds with nearly linear An–O–C angles. Similar trends have been observed in the structural chemistry of early transition metal alkoxide and aryloxide compounds, where short M–O bonds and large M–O–C angles have been taken as structural evidence for oxygen-to-metal π-donation from alkoxide or aryloxide ligands.[43] We note that theoretical and spectroscopic studies have shown that empty thorium 6d orbitals are very low-lying[45] and therefore available for M–O π-bonding interactions. Discrete Variational $X\alpha$ molecular orbital calculations have also revealed uranium 6d involvement in U–O π-bonding in $U(OMe)_6$[46] and U–N π-bonding in the amido and imido ligands of $(RN)U(NR_2)_3$ complexes.[47] In addition, the fact that $Th(O\text{-}2,6\text{-}Me_2C_6H_3)_4(py)_2$ adopts a cis geometry can be interpreted in terms of the maximization of oxygen lone-pair π-donation to the empty metal-based 6d orbitals.

Experimental Section

General Procedures and Techniques. All manipulations were carried out under an inert atmosphere of oxygen-free UHP-grade argon using standard Schlenk techniques or under oxygen-free helium in a Vacuum Atmospheres glovebox. Thorium-232 metal (99.99%) was obtained from Los Alamos National Laboratory stock and machined into turnings. $ThI_4(THF)_4$ and $ThBr_4(THF)_4$ were prepared by dissolution of thorium metal turnings into a THF solution of elemental halogen as described elsewhere.[23] Potassium aryloxide salts were prepared from KH and the appropriate alcohols in THF at room temperature. Sodium hexamethyldisilylamide, $NaN(SiMe_3)_2$, was prepared by a modification of Krüger and Niederprüm.[48] Solvents, except for pyridine, were degassed and distilled from Na/K alloy under nitrogen. Pyridine was distilled from CaH_2 under argon. Benzene-d_6 was degassed, dried over Na/K alloy, and then trap-to-trap distilled before use. Toluene-d_8 was degassed and stored over a potassium mirror. Dichloromethane-d_2 was dried over CaH_2 and trap-to-trap distilled. Solvents were taken into a Vacuum Atmospheres glovebox, and a small amount was tested with a solution of sodium benzophenone in THF. Solvents that failed to maintain a purple coloration from this test were not used.

NMR spectra were recorded on Brüker WM 300 or AF 250 spectrometers in benzene-d_6, toluene-d_8, or dichloromethane-d_2. All ^1H NMR chemical shifts are reported in ppm relative to the ^1H impurity in benzene-d_6, toluene-d_8, or dichloromethane-d_2 set at δ 7.15, 2.09, or 5.32 ppm, respectively. NMR spectra of paramagnetic uranium species are highly temperature dependent; thus it is important to note that the temperatures quoted represent average room temperatures and are approximate values. Infrared spectra were recorded on a Perkin-Elmer 1500 spectrophotometer interfaced with a 1502 Central Processor or on a Digilab FTS-40 spectrophotometer as Nujol mulls between KBr salt plates. Elemental analyses were performed on a Perkin-Elmer 2400 CHN analyzer. Elemental analysis samples were prepared and sealed in tin capsules in the glovebox prior to combustion. Solution UV/visible spectra were recorded under argon using a Perkin-Elmer Lambda 9 spectrophotometer. Electrochemical measurements were obtained using a PAR/EG&G Model 73 potentiostat and Model 175 programmer, with a Houston Instruments Model 1000 XY recorder. Potentials were referenced to Cp_2Fe. Voltammograms were run in a glovebox in a standard H-cell with a 0.1 M $[TBA][BF_4]$/THF solvent system. The working and counter electrodes were of platinum, and the quasi reference electrode was a silver wire separated from the bulk solutions by a fine-porosity glass frit. Ferrocene in the bulk solution was used as an internal potential standard.

Syntheses. A. $\{[(Me_3Si)_2N]_2\overline{Th(CH_2SiMe_2NSiMe_3)}\}$ **(1).** To a solution of 10.00 g (11.82 mmol) of $ThBr_4(THF)_4$ in 150 mL of toluene in a 250-mL Schlenk flask was added 8.67 g (47.30 mmol) of sodium bis(trimethylsilyl)amide as a solution in 30 mL of toluene. A cream-colored suspension formed as the solutions were mixed. The Schlenk reaction vessel was sealed, removed from the drybox, and attached to a Schlenk line. Under an argon purge, a reflux condenser was fitted to the flask, and the contents of the flask were refluxed under argon for a period of 6 h. The flask was sealed and taken into the drybox, and the hot suspension was filtered through a Celite pad on a medium-porosity frit to produce a clear pale-yellow filtrate. All solvent was removed in vacuo to leave a pale-yellow solid, which was dissolved in the minimum quantity of hexane (ca. 125 mL), and the solution was cooled to −40 °C. A mass of off-white needles was deposited after 12 h, these were collected by vacuum filtration through a medium frit, and the filtrate was returned to the freezer to collect two further crops of crystals. The yield was typically 80%.

B. $\{[(Me_3Si)_2N]_2\overline{U(CH_2SiMe_2NSiMe_3)}\}$ **(2).** Following the method of Dormond et al.,[49] 7.46 g (19.6 mmol) of UCl_4 was refluxed with 14.4 g (78.5 mmol) of $Na[N(SiMe_3)_2]$ in 150 mL of toluene for 6 h. Workup procedure was identical to that described for **1**. Yield 8.5 g (60%).

C. $U[O\text{-}2,6\text{-}t\text{-}Bu_2C_6H_3][N(SiMe_3)_2]_3$ **(3).** In a 50-mL Erlenmeyer flask inside the glovebox, 0.50 g (0.70 mmol) of **2** was dissolved in 20 mL of hexane. While the solution was being stirred, 0.14 g (0.68 mmol) of HO-2,6-t-$Bu_2C_6H_3$ in 5 mL of hexane was slowly added via pipet. The color slowly changed from yellow to orange-yellow over the course of several minutes. After being stirred for 12 h, the solvent was removed in vacuo to give a yellow powder. Recrystallization from THF produced large orange cubic crystals after several days at −40 °C. The crystals were collected by decantation and dried under vacuum. A second crop was obtained by further reducing the volume of the solution and cooling. Total yield 0.50 g (79%). Anal. Calcd for $C_{32}H_{75}N_3OSi_6U$: C, 41.57; H, 8.18; N, 4.55. Found: C, 41.59; H, 8.00; N, 4.45. ^1H NMR (22 °C, 250 MHz, C_6D_6): δ 16.5 (s, 2 H, meta-H), 15 (s, 18 H, t-Bu), 13 (s, 1 H, para-H), 3.5 (s, 18 H, SiMe_3), −8 (s, 18 H, SiMe_3), −22.1 (s, 18 H, SiMe_3).

D. $U[O\text{-}2,6\text{-}i\text{-}Pr_2C_6H_3][N(SiMe_3)_2]_3$ **(4).** Using a procedure similar to that for the preparation of **3**, a sample of the metallacycle **2** was treated with 1 equiv of HO-2,6-i-$Pr_2C_6H_3$ in hexane at room temperature. Removal of solvent and recrystallization of the residue from hexanes yielded orange crystals of **4** in 70% yield. Anal. Calcd for $C_{30}H_{71}N_3OSi_6U$: C, 40.20; H, 7.98; N, 4.69. Found: C, 39.62; H, 7.64; N, 4.44. ^1H NMR of this species at room temperature is broad and uninformative. A very broad resonance can be seen for the $[N(SiMe_3)_2]$ groups at δ −7.64.

E. $Th[O\text{-}2,6\text{-}t\text{-}Bu_2C_6H_3][N(SiMe_3)_2]_3$ **(5).** In the glovebox, a 125-mL Erlenmeyer flask was charged with 1.50 g (2.11 mmol) of **1**, a stir bar, and 75 mL of toluene to give a pale-yellow solution. Then 0.45 g (2.18 mmol) of HO-2,6-t-$Bu_2C_6H_3$ was dissolved in 5 mL of toluene, and the resulting solution was added dropwise to the stirring thorium metallacycle solution. After the reaction mixture was stirred for 6 h at room temperature, toluene was removed in vacuo and the solid white residue taken into 100 mL of hexane. The resulting hexane solution was filtered, reduced in volume to ca. 40 mL, and cooled to −40 °C overnight to yield colorless crystals of **5** which were isolated by vacuum filtration. Yield 1.52 g (79%). Anal. Calcd for $C_{32}H_{75}N_3OSi_6Th$: C, 41.84; H, 8.23; N, 4.57. Found: C, 41.62; H, 7.81; N, 4.52. ^1H NMR (22 °C, 250 MHz, C_6D_6): δ 7.28 (d, 2 H, $^3J_{HH}$ = 8 Hz, meta-H), 6.80 (t, ^1H, $^3J_{HH}$ = 8 Hz, para-H), 1.66 (s, 18 H, t-Bu), 0.44 (s, 54 H, $N(SiMe_3)_2$). IR (Nujol, cm^{-1}): 1400 (s), 1388 (s), 1248 (vs), 1218 (s), 1210 (s), 1198 (s), 1124 (m), 896 (vs), 856 (vs), 838 (vs), 818 (s), 790 (sh, m), 776 (s), 746 (m), 690 (m), 666 (s), 656 (sh, m), 612 (s).

F. $Th[O\text{-}2,6\text{-}Me_2C_6H_3][N(SiMe_3)_2]_3$ **(6).** In the glovebox, a 125-mL Erlenmeyer flask was charged with 1.50 g (2.11 mmol) of metallacycle **1**, and 75 mL of toluene was added. Next, 0.27 g (2.21 mmol) of HO-2,6-$Me_2C_6H_3$ (dissolved in 10 mL of toluene) was added dropwise with stirring via pipet. This solution was stirred for 12 h, and then all solvent was removed under reduced pressure to leave a white solid. This solid was recrystallized from 30 mL of hexane at −40 °C to yield 1.56

(44) We envision that this reaction could proceed via $\{U(H)(OAr^*)_3[N(SiMe_3)_2]\}^+(OAr^*)^-$.

(45) Bursten, B. E.; Rhodes, L. R.; Strittmatter, R. J. *J. Less-Common Met.* **1989**, *149*, 207. Ionova, G. V.; Pershina, V. G.; Spitsyn, V. I. *Dokl. Akad. Nauk SSSR* **1982**, *263*, 130. Hessler, J. P.; Carnall, W. T. In *Lanthanide and Actinide Chemistry and Spectroscopy*; Edelstein, N. M., Ed.; American Chemical Society: Washington, D.C., 1980.

(46) Bursten, B. E.; Casarin, M.; Ellis, D. E.; Fragala, I.; Marks, T. J. *Inorg. Chem.* **1986**, *25*, 1257.

(47) Bowmaker, G. A.; Görling, A.; Häberlen, O.; Rösch, N.; Goodman, G. L.; Ellis, D. E. *Inorg. Chem.* **1992**, *31*, 577.

(48) Krüger, C. R.; Niederprüm, H. *Inorg. Synth.* **1966**, *8*, 15.

(49) Dormond, A.; El Bouadili, A.; Aaliti, A.; Moise, C. *J. Organomet. Chem.* **1985**, *288*, C1.

g (89%) of colorless crystals of **6**. Anal. Calcd for $C_{26}H_{63}N_3OSi_6Th$: C, 37.43; H, 7.61; N, 5.04. Found: C, 35.74; H, 6.47; N, 4.53. ^1H NMR (22 °C, 250 MHz, C_6D_6): δ 7.01 (d, 2 H, $^3J_{HH}$ = 7 Hz, meta-H), 6.75 (t, 1 H, $^3J_{HH}$ = 7 Hz, para-H), 2.46 (s, 6 H, Me), 0.38 (s, 54 H, $N(SiMe_3)_2$). IR (Nujol mull): 1595 (m), 1428 (sh, s), 1403 (sh, m), 1287 (sh, m), 1267 (s), 1252 (s), 1221 (s), 1109 (w), 1091 (s), 1033 (w), 921 (s), 842 (s), 774 (s), 759 (s), 733 (m), 714 (m), 666 (s), 611 (s), 560 (w), 541 (m), 489 (w).

G. Th[*O*-2,6-*t*-$Bu_2C_6H_3$]$_2$[$N(SiMe_3)_2$]$_2$ (7). **1** (3.50 g, 4.91 mmol) was dissolved in 100 mL of toluene in a Schlenk reaction vessel, and then 3.05 g (14.8 mmol) of HO-2,6-*t*-$Bu_2C_6H_3$ was added as a solution in toluene. The flask was attached to a Schlenk line, and the contents were refluxed under argon for 6 h, before being returned to the drybox. All solvent was removed in vacuo to leave a pale-yellow solid, which was dissolved in 100 mL of hexane/toluene (1:1) and vacuum-filtered through a Celite pad on a medium-porosity frit. The volume of the filtrate was reduced to ca. 20 mL, and the filtrate was cooled to −40 °C to yield, over several days, colorless crystals of **7**, which were decanted free from solvent and allowed to dry. Yield 2.20 g (46%). Anal. Calcd for $C_{40}H_{78}N_2O_2Si_4Th$: C, 49.87; H, 8.16; N, 2.91. Found: C, 49.85; H, 8.18; N, 2.79. ^1H NMR (22 °C, 250 MHz, C_6D_6): δ 7.23 (d, 2 H, $^3J_{HH}$ = 7 Hz, meta-H), 6.78 (t, 1 H, $^3J_{HH}$ = 7 Hz, para-H), 1.56 (s, 18 H, *t*-Bu), 0.47 (s, 18 H, $N(SiMe_3)_2$). IR (Nujol, cm^{-1}): 1402 (s), 1360 (m), 1254 (s), 1248 (s, sh), 1220 (s), 1210 (s), 1196 (s), 1124 (m), 896 (s), 856 (s), 838 (s), 818 (s), 776 (m), 748 (s), 690 (w), 664 (s), 656 (s), 614 (s), 560 (w), 550 (w).

H. Th[*O*-2,6-*t*-$Bu_2C_6H_3$]$_3$[$N(SiMe_3)_2$] (8). In the drybox, 1.50 g (2.11 mmol) of thorium metallacycle **1** was dissolved in 100 mL of toluene in a Schlenk reaction vessel and 1.52 g (7.37 mmol) of HO-2,6-*t*-$Bu_2C_6H_3$ added as a solution in toluene. The flask was removed from the drybox and attached to a Schlenk line, and the reaction mixture was refluxed for 12 h under argon before being returned to the drybox. All solvent was removed in vacuo to leave a pale-yellow solid, which was dissolved in 75 mL of 1:1 hexane/toluene; the resulting solution was filtered through Celite and the filtrate reduced in volume to 20 mL. Cooling to −40 °C yielded pale-yellow crystals of **8** over a period of days. The crystals were isolated by decantation and allowed to dry under a helium atmosphere. Yield 1.38 g (65%). Anal. Calcd for $C_{48}H_{79}NO_3Si_2Th$: C, 57.29; H, 7.91; N, 1.39. Found: C, 58.35; H, 6.73; N, 1.45. ^1H NMR (22 °C, C_6D_6): δ 7.25 (d, 2 H, $^3J_{HH}$ = 8 Hz, meta-H), 6.80 (t, 1 H, $^3J_{HH}$ = 8 Hz, para-H), 1.59 (s, 18 H, *t*-Bu), 0.36 (s, 6 H, $N(SiMe_3)_2$). IR (Nujol, cm^{-1}): 1404 (s), 1364 (m), 1340 (w), 1264 (m), 1254 (m), 1216 (s), 1208 (s), 1196 (s), 1122 (m), 908 (s), 878 (m), 854 (s), 834 (m), 818 (m), 792 (w), 776 (m), 746 (s), 654 (m), 616 (w), 560 (w), 546 (w).

I. Th(*O*-2,6-*t*-$Bu_2C_6H_3$)$_4$ (9). In the glovebox, $ThI_4(THF)_4$ (7.00 g, 6.81 mmol) was dissolved in 150 mL of THF in a 250-mL Erlenmeyer flask, and then potassium 2,6-di-*tert*-butylphenoxide (6.86 g, 28.1 mmol) was slowly added as a solid over a period of 10 min. The resulting white suspension was allowed to stir at room temperature for 24 h, before being filtered through Celite using a coarse-porosity frit. All solvent was removed from the filtrate in vacuo to leave an off-white solid, to which was added 100 mL of hot (60 °C) toluene to extract the product. The toluene extract was filtered through Celite once more, before the toluene was removed in vacuo to leave an off-white powder. Yield 7.05 g (98%). The product may be recrystallized from toluene. Anal. Calcd for $C_{56}H_{84}O_4Th$: C, 63.86; H, 8.04. Found: C, 64.86; H, 8.38. ^1H NMR (22 °C, C_6D_6): δ 7.25 (d, 2 H, $^3J_{HH}$ = 8 Hz, meta-H), 6.82 (t, 1 H, $^3J_{HH}$ = 8 Hz, para-H), 1.58 (s, 18 H, *t*-Bu). $^{13}C\{^1H\}$ NMR (22 °C, 62.9 MHz, CD_2Cl_2): δ 161.8 (s, ipso-C), 137.9 (s, ortho-C), 126.3 (s, meta-C), 119.9 (s, para-C), 35.6 (s, $C(CH_3)_3$), 33.4 (s, $C(CH_3)_3$). IR (Nujol, cm^{-1}): 1576 (w), 1406 (s), 1388 (m), 1356 (w), 1300 (m), 1266 (w), 1210 (s), 1196 (s), 1120 (m), 1096 (m), 880 (w), 856 (s), 818 (m), 794 (w), 756 (s), 750 (sh, m), 656 (s).

J. Th(*O*-4-*t*-BuC_6H_4)$_4$(py)$_3$ (10). In the glovebox, 2.00 g (2.81 mmol) of thorium metallacycle **1** was dissolved in 100 mL of toluene in a 125-mL Erlenmeyer flask, and then 1.69 g (11.25 mmol) of HO-4-*t*-BuC_6H_4 was added slowly as a slurry in 10 mL of toluene. A white precipitate formed as the phenol was added to the metallacycle. This suspension was stirred for 24 h, and then 4 mL of pyridine was added, causing the solid to dissolve completely. The volume of the solution was reduced to 80 mL, at which point a white solid started to precpitate. This solution was placed at −40 °C overnight to produce a white microcrystalline solid, which was collected by vacuum filtration, washed with hexane, and dried in vacuo. Yield 2.48 g (83%). Anal. Calcd for $C_{55}H_{67}N_3O_4Th$: C, 61.96; H, 6.33; N, 3.94. Found: C, 62.02; H, 5.91; N, 4.37. ^1H NMR (22 °C, C_6D_6): δ 8.54 (d, 6 H, $^3J_{HH}$ = 3 Hz, ortho-py), 7.13 (m, 8 H, ortho- or meta-OC_6H_4-*t*-Bu), 6.98 (br m, 8 H, meta- or ortho-OC_6H_4-*t*-Bu), 6.82 (t, 3 H, $^3J_{HH}$ = 5 Hz, para-py), 6.51 (m, 6 H, meta-py), 1.25 (s, 36 H, *t*-Bu). IR (Nujol, cm^{-1}): 1598 (s), 1574 (sh, w), 1504 (s), 1484 (sh, m), 1442 (s), 1362 (m), 1284 (vs), 1266 (s), 1216 (w), 1174 (m), 1150 (w), 1106 (w), 1070 (w), 1036 (m), 1004 (m), 864 (s), 834 (s), 754 (w), 726 (w), 700 (s), 684 (s), 620 (m), 556 (m), 530 (m).

K. U(*O*-2,6-*t*-$Bu_2C_6H_3$)$_4$ (11). In a Schlenk reaction vessel equipped with a reflux condenser, 1.16 g (5.57 mmol) of HO-2,6-*t*-$Bu_2C_6H_3$ was added to a toluene solution containing 1.00 g (1.39 mmol) of **2**. The solution was heated at reflux for 12 h, after which the solvent was removed in vacuo to produce an orange oily solid. Recrystallization from THF produced large orange crystals (0.96 g, 65%). Anal. Calcd for $C_{56}H_{84}O_4U$: C, 63.50; H, 7.99; N, 0.00. Found: C, 63.53; H, 7.82; N, <0.05. ^1H NMR (22 °C, C_6D_6): δ 10.5 (d, 2 H, meta-H), 8.3 (t, 1 H, para-H), −1.0 (br s, 18 H, *t*-Bu). IR (Nujol, cm^{-1}): 535 (w), 544 (m), 561 (m), 633 (m), 656 (s), 750 (s), 795 (ms), 818 (s), 852 (s), 880 (ms), 1119 (ms), 1190 (s, br), 1205 (ms), 1267 (ms), 1387 (s), 1402 (vs), 1483 (ms), 1578 (w), 1584 (mw).

L. U(*O*-2,6-*i*-$Pr_2C_6H_3$)$_4$ (12). In the drybox, 1.40 g (1.95 mmol) of uranium metallacycle **1** was dissolved in 75 mL of toluene in a 125-mL Schlenk reaction vessel, and a stir bar was added. Then a solution of 1.40 g (7.85 mmol) of 2,6-diisopropylphenol in 10 mL of toluene was added to the stirring uranium solution, resulting in a color change from orange-brown to pale orange. The flask was sealed, removed from the drybox, and attached to a Schlenk line. A reflux condenser was attached to the flask, and the contents were refluxed under argon for 6 h. The resulting deep orange-brown solution was returned to the drybox and stripped to dryness under reduced pressure. The dark-brown solid residue was extracted into 75 mL of hexane, and the resulting solution was filtered through Celite on a medium frit. The volume of the filtrate was reduced to 20 mL and placed in a vial in the freezer at −40 °C. Overnight, dark-orange-brown crystals were deposited. These were decanted free from solvent and allowed to dry in the box atmosphere. Yield 0.77 g (42%). Anal. Calcd for $C_{48}H_{68}O_4U$: C, 60.87; H, 7.24. Found: C, 61.06; H, 8.16. ^1H NMR (22 °C, C_6D_6): δ 11.5 (br, 2 H, meta-H), 9.9 (br, 1 H, para-H), 1.1 (br, 2 H, $CHMe_2$), −0.4 (br s, 12 H, $CHMe_2$).

M. Th(*O*-2,6-$Me_2C_6H_3$)$_4$(THF)$_2$ (13). $ThI_4(THF)_4$ (5.20 g, 5.06 mmol) was dissolved in 150 mL of THF and then 3.30 g (20.6 mmol) of potassium 2,6-dimethylphenoxide added as a solid over a period of 10 min. The resulting white suspension was allowed to stir at room temperature for 24 h, before being filtered through Celite on a coarse-porosity frit. All solvent was removed from the filtrate in vacuo to leave a pale-pink solid, to which was added 150 mL of hexane with shaking. This resulted in a pale-pink solution and an off-white solid. The hexane slurry was filtered through a medium-porosity frit, and the product was collected on the frit and pumped dry. Yield 3.08 g (71%). Anal. Calcd for $C_{40}H_{52}O_6Th$: C, 55.81; H, 6.09. Found: C, 56.89; H, 5.60. ^1H NMR (22 °C, C_6D_6): δ 7.08 (d, 2 H, $^3J_{HH}$ = 7 Hz, meta-H), 6.78 (t, 1 H, $^3J_{HH}$ = 7 Hz, para-H), 3.72 (m, 2 H, α-THF), 2.35 (s, 6 H, $Me_2C_6H_3$), 1.12 (m, 2 H, β-THF). IR (Nujol, cm^{-1}): 1590 (m), 1424 (s), 1294 (m), 1272 (s), 1230 (s), 1090 (m), 1014 (w), 916 (w), 856 (s), 758 (m), 742 (w), 704 (m), 538 (m).

N. Th(*O*-2,6-*i*-$Pr_2C_6H_3$)$_4$(THF)$_2$ (14). $ThI_4(THF)_4$ (7.00 g, 6.81 mmol) was dissolved in 150 mL of THF and then 6.06 g (28.0 mmol) of potassium 2,6-diisopropylphenoxide added as a solid over a period of 10 min to produce a white suspension. This was allowed to stir at room temperature for 24 h, before being filtered through a Celite pad on a coarse-porosity frit. All solvent was removed from the filtrate in vacuo to leave a pale-orange solid, to which was added 150 mL of hexane. This produced a pale-orange solution and a white solid. The hexane extract was filtered through a medium-porosity frit, and the product remaining on the frit was pumped dry. A further crop of solid was obtained by cooling the hexane filtrate to −40 °C. Yield 4.50 g (61%). Anal. Calcd for $C_{56}H_{84}O_6Th$: C, 61.97; H, 7.80. Found: C, 62.04; H, 7.86. ^1H NMR (22 °C, C_6D_6): δ 7.12 (d, 2 H, $^3J_{HH}$ = 8 Hz, meta-H), 6.91 (t, 1 H, $^3J_{HH}$ = 8 Hz, para-H), 3.94 (m, 2 H, α-THF), 3.63 (septet, 2 H, $^3J_{HH}$ = 7 Hz, $CHMe_2$), 1.32 (m, 2 H, β-THF), 1.20 (d, 12 H, $^3J_{HH}$ = 7 Hz, $CHMe_2$). IR (Nujol, cm^{-1}): 1590 (m), 1434 (s), 1360 (w), 1326 (s), 1254 (s), 1196 (s), 1116 (w), 1100 (m), 1058 (w), 1044 (m), 1018 (m), 936 (w), 886 (m), 860 (s), 846 (s), 796 (w), 752 (s), 694 (s), 568 (s).

O. Th(*O*-2,6-$Me_2C_6H_3$)$_4$(py)$_2$ (15). Th(*O*-2,6-$Me_2C_6H_3$)$_4$(THF)$_2$ (**13**) (1.50 g, 1.74 mmol) was dissolved in 40 mL of toluene, and 2 mL of pyridine was added. After the reaction mixture was stirred for 18 h at room temperature, all solvent was removed in vacuo and the residue recrystallized from toluene at −40 °C to give pale-brown crystals of the bis(pyridine) adduct **15**. Yield 1.00 g (66%). Anal. Calcd for $C_{42}H_{46}N_2O_4Th \cdot C_7H_8$: C, 60.86; H, 5.63; N, 2.90. Found: C, 61.21; H, 5.75; N, 3.34. ^1H NMR (22 °C, C_6D_6): δ 8.65 (m, 2 H, ortho-NC_5H_5), 7.05 (d, 4 H, $^3J_{HH}$ = 7 Hz, meta-C_6H_3), 6.77 (t, 2 H, $^3J_{HH}$ = 7 Hz, para-C_6H_3), 6.70 (t, 1 H, $^3J_{HH}$ = 8 Hz, para-NC_5H_5), 6.32 (m, 2 H, meta-NC_5H_5), 2.19 (s, 12 H, $Me_2C_6H_3$). IR (Nujol, cm^{-1}): 1600 (m), 1590 (m), 1444 (s), 1422 (m), 1294 (m), 1272 (s), 1230 (s), 1158 (w),

1090 (m), 1070 (w), 1038 (m), 1006 (m), 982 (w), 916 (w), 870 (s), 856 (s), 772 (sh, m), 760 (s), 742 (m), 730 (m), 704 (s), 626 (m), 536 (s).

P. [2,6-*t*-$Bu_2C_6H_3O$][$(Me_3Si)_2N$]UN(SiMe$_3$)SiMe$_2$CH$_2$ (16). In a sealed 5-mm NMR tube U[*O*-2,6-*t*-$Bu_2C_6H_3$][$N(SiMe_3)_2$]$_3$ (50 mg, 6.6 × 10^{-2} mmol) was heated in benzene-d_6 at 60 °C. The course of the reaction was periodically monitored by ^{1}H NMR, but there was no observable color change. After the reaction was complete (12 h, by ^{1}H NMR), the NMR tube was brought back into the drybox and the seal was broken with a file, the solution was poured into a flask, and the volatiles were removed in vacuo to yield a yellow solid. The yellow solid was redissolved in benzene-d_6 and a final ^{1}H NMR spectrum obtained. The yield was nearly quantitative on the basis of ^{1}H NMR (Figure 5). On the basis of ^{1}H NMR, there appears to be a small amount of another compound formed in this reaction which may be the result of cyclometalation of the phenoxide *t*-Bu group. The solvent was again removed in vacuo and the resulting yellow solid sealed in a tin capsule for elemental analysis. Anal. Calcd for $C_{26}H_{56}N_2OSi_4U$: C, 40.92; H, 7.40; N, 3.67. Found: C, 40.63; H, 7.07; N, 3.16. ^{1}H NMR (22 °C, 250 MHz, C_6D_6): δ 16.1 (s, 2 H, meta-H), 13.1 (s, 1 H, para-H), 11.3, 11.0 (s, 2 × 3 H, $SiMe_2$), 3.6 (s, 9 H, $N(SiMe_3)$), −5.6 (s, 18 H, *t*-Bu), −15.4 (s, 18 H, $N(SiMe_3)_2$), −151.2, −191.9 (s, 2 × 1 H, CH_2).

Q. [2,6-*t*-$Bu_2C_6H_3O$][$(Me_3Si)_2N$]ThN(SiMe$_3$)SiMe$_2$CH$_2$ (17). The procedure was similar to that used to prepare **16** except that a sample of **5** was dissolved in benzene-d_6 and heated to 110 °C for 3 h. ^{1}H NMR (C_6D_6, 250 MHz, 22 °C): δ 7.24 (d, 2 H, $^3J_{HH}$ = 8 Hz, meta-H), 6.83 (t, 1 H, $^3J_{HH}$ = 8 Hz, para-H), 1.50 (s, 18 H, *t*-Bu), 1.20 (br s, 2 H, CH_2), 0.36 (s, 18 H, $N(SiMe_3)_2$), 0.33 (s, 6 H, $SiMe_2$), 0.26 (s, 9 H, $SiMe_3$).

Crystallographic Studies. A summary of crystallographic data can be found in Table I. General operating procedures have been described elsewhere.[50]

A. U[*O*-2,6-*t*-$Bu_2C_6H_3$][$N(SiMe_3)_2$]$_3$ (3). A suitable fragment was cleaved from a larger single crystal, transferred to the goniostat using standard inert-atmosphere handling techniques employed by the IUMSC, and cooled to −155 °C for characterization and data collection.

A systematic search of a limited hemisphere of reciprocal space located a set of diffraction maxima with symmetry and systematic absences corresponding to the unique orthorhombic space group $P2_12_12_1$. Subsequent solution and refinement of the structure confirmed this choice. Data were collected in the usual manner using a continuous θ–2θ scan with fixed backgrounds. Data were reduced to a unique set of intensities and associated sigmas in the usual manner. The structure was solved by a combination of direct methods (MULTAN78) and Fourier techniques. Hydrogen atoms were introduced in fixed positions, and refinement was completed after the data were corrected for absorption.

A final difference Fourier was featureless, with the largest peak being 1.0 e/Å^3, located adjacent to the uranium atom. The absolute configuration was determined by examination of the residuals for the two possible chiral forms.

B. Th[*O*-2,6-*t*-$Bu_2C_6H_3$]$_4$ (9). The crystal selected for study was mounted on a glass fiber using silicone grease and was transferred to a goniostat where it was cooled to −171 °C for characterization and data collection. The air-sensitive crystals were kept under a nitrogen atmosphere using standard glovebag techniques.

A systematic search of a limited hemisphere of reciprocal space revealed a tetragonal cell with systematic extinctions corresponding to a body-centered system. An initial assignment of $I\bar{4}$ proved to be the correct space group, on the basis of subsequent solution and refinement. Data were collected using a standard moving crystal–moving detector technique, and after correction for background, Lorentz, and polarization terms, the data were averaged to yield a unique set of intensities. An attempt to correct the data for absorption failed to improve the *R* for averaging, and on the basis of the small size and poor definition of faces, the absorption correction was dismissed.

Direct methods revealed the metal atom to be at the origin and a second atom, assigned as oxygen, was used in the phasing to locate the remainder of the non-hydrogen atoms. A difference Fourier located most of the hydrogen atoms, but when attempts were made to refine their positions, several were poorly behaved and failed to converge. For this reason, all hydrogen atoms were placed in idealized and fixed positions for the remainder of the refinement in which all non-hydrogen atoms were refined anisotropically.

A final difference Fourier was featureless, with one peak of 1.2 e/Å^3 at the origin and all other peaks being less than 0.42 e/Å^3.

C. U[*O*-2,6-*t*-$Bu_2C_6H_3$]$_4$ (11). The crystal selected for study was mounted using silicone grease and was transferred to a goniostat where it was cooled to −145 °C for characterization and data collection. A systematic search of a limited hemisphere of reciprocal space revealed $4/m$ Laue symmetry with systematic absences indicating *I* centering. Data processing gave a residual of 0.065 for 2026 unique intensities, all of which were measured more than once during data collection. Four standards measured every 300 data points showed no systematic trends. No correction was made for absorption.

The structure was solved by a combination of Patterson map analysis and Fourier techniques. The Patterson map was consistent with a uranium atom at the origin with tetrahedral bonding to the uranium. This led to a choice of $I\bar{4}$ for the space group, which proved to be correct by the successful solution of the structure. After the non-hydrogen atoms had been located and refined, a difference map revealed positions for most of the hydrogen atoms. All of the hydrogen atoms were predictable and were placed in idealized positions prior to the final least-squares cycles in which the non-hydrogen atoms were refined with anisotropic thermal parameters and the hydrogen atoms were refined with isotropic thermal parameters. Although the resulting hydrogen positions were qualitatively correct, for clarity they were given idealized positions and thermal parameters in the figure.

The final least-squares cycles had a $R(F)$ = 0.029. The final difference Fourier had residual peaks of 1 e/Å^3 near the uranium position. All other residual peaks were 0.5 e/Å^3 or less.

D. Th[*O*-2,6-$Me_2C_6H_3$]$_4$(py)$_2$ (15). The air-sensitive sample was placed in a nitrogen-filled glovebag, and a small crystal was affixed to a glass fiber on a goniometer head. The crystal was then transferred to the diffractometer where it was cooled to −171 °C for characterization and data collection.

A systematic search of a limited hemisphere of reciprocal space located a set of diffraction maxima with symmetry and systematic absences corresponding to the unique monoclinic space group $P2_1/n$. Subsequent solution and refinement confirmed this choice. Data were collected using a standard moving crystal–moving detector technique, and after correction for background, Lorentz, and polarization terms, the data were averaged to yield a unique set of intensities.

The thorium atom was located using a Patterson synthesis, and all other atoms were located in subsequent Fourier syntheses. Hydrogen atoms were placed in fixed idealized positions for the final cycles of refinement.

Acknowledgment. We thank Drs. C. J. Burns and B. E. Bursten for helpful discussions and Dr. W. H. Smith, Miss D. E. Smith, Dr. D. M. Barnhart, and Miss T. M. Frankcom for technical assistance. We acknowledge the Office of Basic Energy Sciences, Division of Chemical Sciences, U.S. Department of Energy, under Contract Number W-7405-eng-36, and the Yucca Mountain Site Characterization Project Office for financial support.

Supplementary Material Available: Tables of atomic positional parameters and anisotropic thermal parameters for An(*O*-2,6-*t*-$Bu_2C_6H_3$)[$N(SiMe_3)_2$]$_3$ (**3**), Th(*O*-2,6-*t*-$Bu_2C_6H_3$)$_4$ (**9**), U(*O*-2,6-*t*-$Bu_2C_6H_3$)$_4$ (**11**), and Th(*O*-2,6-$Me_2C_6H_3$)$_4$(py)$_2$ (**15**) (22 pages); listing of observed and calculated structure factors for **3**, **9**, **11**, and **15** (30 pages). Ordering information is given on any current masthead page.

(50) Chisholm, M. H.; Folting, K.; Huffman, J. C.; Kirkpatrick, C. C. *Inorg. Chem.* **1984**, *23*, 1021.